



Royal Netherlands Institute for Sea Research

This is a preprint of:

Warden, L., Meer, M.T.J. van der, Moros, M. & Sinninghe Damsté, J.S. (2016). Sedimentary alkenone distributions reflect salinity changes in the Baltic Sea over the Holocene. *Organic Geochemistry*, 102, 30-44

Published version: [dx.doi.org/10.1016/j.orggeochem.2016.09.007](https://doi.org/10.1016/j.orggeochem.2016.09.007)

Link NIOZ Repository: www.vliz.be/nl/imis?module=ref&refid=281227

Article begins on next page]

The NIOZ Repository gives free access to the digital collection of the work of the Royal Netherlands Institute for Sea Research. This archive is managed according to the principles of the [Open Access Movement](#), and the [Open Archive Initiative](#). Each publication should be cited to its original source - please use the reference as presented.

When using parts of, or whole publications in your own work, permission from the author(s) or copyright holder(s) is always needed.

Sedimentary alkenone distributions reflect salinity changes in the Baltic Sea over the Holocene

Lisa Warden¹, Marcel T.J. van der Meer¹, Matthias Moros², and Jaap S. Sinninghe Damsté^{1,3,*}

¹ *NIOZ Netherlands Institute for Sea Research, Department of Marine Microbiology and Biogeochemistry, and Utrecht University, PO Box 59, 1790 AB Den Burg, the Netherlands.*

² *The Leibniz Institute for Baltic Sea Research, Department of Marine Geology, Warnemünde, Germany.*

³ *Utrecht University, Faculty of Geosciences, P.O. Box 80.021, 3508 TA Utrecht, The Netherlands.*

* corresponding author: jaap.damste@nioz.nl

1 **Abstract**

2 The Baltic Sea has had a complex salinity history since the last deglaciation. Here we show
3 how distributions and concentrations of alkenones and their δD values varied with past
4 fluctuations in salinity in the Baltic Sea over the Holocene by examining a Holocene record
5 (11.2 to 0.1 cal kyr BP) from the Arkona Basin. Major changes in the alkenone distribution,
6 i.e. changes in the fractional abundance of the $C_{37:4}$ alkenone, the $C_{38:2}$ Et alkenones and the
7 $C_{36:2}$ alkenone, the latter which has not been reported in the Baltic Sea previously, correlated
8 with known changes in salinity. Both alkenone distributions and hydrogen isotopic
9 composition suggest a shift in haptophyte species composition from lacustrine to brackish
10 type haptophytes around 7.7-7.2 cal kyr BP, corresponding with a salinity change that
11 occurred when the connection between the basin and the North Sea was re-established. A
12 similar salinity change occurred in the Black Sea making it possible to directly compare and
13 use the δD values and alkenone distributions previously published to corroborate the
14 interpretations made about salinity changes from the data presented for the Baltic Sea. Low
15 and variable salinity waters in the Baltic Sea over the Holocene have allowed for alkenones
16 derived from a variable haptophyte community composition, including low salinity adapted
17 species, hindering the use of the unsaturation ratios of long-chain alkenones for sea surface
18 temperature reconstruction. However, these alkenone based indices are potentially useful for
19 studying variations in salinity, regionally as well as in the past.

20

21 **Keywords**

22 alkenones, Baltic Sea, $C_{36:2}$ alkenone, haptophyte community, paleosalinity, δD of alkenones

23 1. Introduction

24 Long chain alkenones, biolipids composed of predominantly C₃₇- C₃₉ n-alkyl chains with
25 di-, tri- or tetra unsaturations and a keto functionality at position C-2 or C-3 (de Leeuw et al.,
26 1980; Rechka and Maxwell, 1988) are produced exclusively by only a few species of
27 haptophyte algae in both open marine (e.g. *Emiliania huxleyi* and *Geophyrocapsa oceanica*;
28 Volkman et al., 1980, 1995) and coastal or lacustrine regions (e.g. *Isochrysis galbana* and
29 *Ruttnera (Chrysothilla) lamellosa*; Marlowe et al., 1984) and the more recently discovered
30 'Greenland haptophyte' species, so far exclusively found in Greenland and Alaskan lakes
31 (D'Andrea et al., 2006). An unusual C₃₆ diunsaturated alkenone was also identified by Xu et
32 al. (2001) in Holocene sediments from the Black Sea and since then Coolen et al. (2009)
33 reported its biological origin in the Black Sea is most likely a specific strain of *E. huxleyi*.

34 Since field sampling and culture experiments demonstrated a relationship between surface
35 water temperature and the unsaturation ratios of long-chain alkenones, the unsaturation ratios
36 of sedimentary alkenones have been extensively used as a paleotemperature proxy (Prahl and
37 Wakeham, 1987; Jensen, 1995; Müller et al., 1998). Two alkenone unsaturation ratios have
38 been predominantly used in sea surface temperature (SST) reconstructions, the U^K₃₇ (which
39 includes the relative abundance of di-, tri- and tetra- unsaturated alkenones; Brassell et al.,
40 1986) and the U^{K'}₃₇ (which excludes the tetra-unsaturated alkenone; Prahl and Wakeham,
41 1987). Even though this proxy has been successfully applied in marine settings, uncertainties
42 still exist due to increasing evidence of non-thermal effects on alkenone distribution patterns
43 such as species and strain composition (Volkman et al., 1995; Conte et al., 1998) and salinity
44 (Chu et al., 2005; Ono et al., 2012; Chivall et al., 2014). For example, Rosell-Melé (1998)
45 demonstrated that the amount of C_{37:4} alkenone compared to the abundance of the other C₃₇
46 alkenones (%C_{37:4}) in particulate organic matter from Nordic Seas had a stronger correlation
47 to sea surface salinity (SSS) than SST. Despite these results, the correlation between salinity

48 and %C_{37:4} in surface water and sediment trap samples worldwide varies greatly and so there
49 is no evidence supporting the application of a linear relationship (Sikes and Sicre, 2002),
50 which would make the use of %C_{37:4} as a salinity proxy possible. However, it has been
51 suggested that if the relative abundance of the C_{37:4} alkenone is over 5% this might be an
52 indicator of alkenone contributions from haptophyte populations adapted to lower salinity
53 conditions (Thiel et al., 1997; Rosell-Melé, 1998; Schulz et al., 2000; Bendle et al., 2005).
54 Therefore, this cut-off value of 5% could be applied when determining if alkenone
55 unsaturation ratios can be used for paleotemperature reconstructions.

56 Alkenones are common biomarkers in marine sediments, but occasionally also occur in
57 lake sediments. In lake settings, such as Lake Van in Turkey (Thiel et al., 1997; Randlett et
58 al., 2014) and Chinese lakes (Chu et al., 2005; Song et al., 2016), complications applying
59 long chain alkenone unsaturation patterns as a temperature proxy have often been noted.
60 Previous studies have found that alkenone biosynthesizing haptophyte algae are much more
61 genetically diverse in lacustrine settings than marine and this could affect alkenone
62 composition and have implications for using alkenone distributions for SST reconstructions
63 (Zink et al., 2001; Sun et al., 2007; Randlett et al., 2014). In a study of 37 lakes in China, Chu
64 et al. (2005) demonstrated that the fractional abundance of the C_{37:4} methyl ketone (i.e. 5-96%
65 of the sum of C₃₇ alkenones) is much higher than has been observed in marine settings and is
66 highly variable in the different lakes, complicating the use of the U^K₃₇ SST proxy. Chu et al.
67 (2005) concluded that, although salinity may be an indirect factor affecting %C_{37:4}, it is
68 probably not the main factor. A more recent study on lakes in northwestern China (Song et al.,
69 2016) also encountered complications using alkenone unsaturation ratios as a
70 paleotemperature proxy finding that salinity has a large influence on the occurrence,
71 concentration and composition of alkenones. The predominance of the C_{37:4} methyl ketone and
72 its negative relationship with salinity indicated that its production is probably a response to

73 low salinity conditions. Consequently, it was suggested that the long chain alkenone
74 unsaturation ratio omitting $C_{37:4}$ ($U_{37}^{K'}$) yields more accurate SST estimations when used in
75 lakes. However, recently a new index has been proposed for lacustrine, brackish and estuarine
76 settings that includes the $C_{37:4}$ alkenone and instead excludes $C_{37:2}$ ($U_{37}^{K''}$; Zheng et al., 2016).
77 This study suggests that the di-unsaturated alkenones play a less important role than the tri-
78 and tetra- in regards to regulating cell functions in accordance with temperature fluctuations
79 in lower salinity settings. Additionally, an absence of C_{38} methyl ketones has been observed
80 in alkenone containing freshwater lakes in China (Song et al., 2016), indicating that perhaps
81 this could be used as a criterion for identifying alkenone producers coming from freshwater
82 environments.

83 Previous studies in brackish settings have shown that since alkenone distributions co-vary
84 with salinity driven changes in haptophyte species composition, the use of long chain
85 alkenones is difficult in areas with low and/or fluctuating salinity such as in the Black Sea
86 (Coolen et al., 2009), Ace Lake in Antarctica (Coolen et al., 2004), the Baltic Sea (Rosell-
87 Melé, 1998; Schulz et al., 2000; Blanz et al., 2005) and the North Atlantic and Nordic Seas
88 (Rosell-Melé, 1998). In Ace Lake, Coolen et al. (2004) demonstrated that as lake chemistry
89 changed over time, particularly the salinity as it evolved from a freshwater basin to a marine
90 inlet, the alkenone distributions changed reflecting differences in the haptophyte population as
91 evident from palaeogenetic signatures. Similarly, in the Black Sea, Coolen et al. (2009)
92 showed that as salinity increased over the Holocene in the basin that the haptophyte
93 composition changed as well resulting in erroneous alkenone-derived SST estimates at times.
94 For the North Atlantic and Nordic Seas, Rosell-Melé (1998) observed that the $\%C_{37:4}$ is
95 related to salinity as well as temperature changes.

96 In addition to these studies, culture experiments have been performed and confirm that
97 alkenone distribution patterns can vary with changing salinity and that this should be taken

98 into account when using the alkenone unsaturation indices for SST reconstructions (Chu et al.,
99 2005; Ono et al., 2012; Chivall et al., 2014). The results from Chivall et al. (2014) indicate
100 salinity has an effect on alkenone distributions, but that other factors such as growth phase
101 and species composition also play a role in whether the long chain alkenone distributions are
102 affected by salinity. This culture study found a positive correlation between %C_{37:4} and
103 salinity, however, they found growth phase has a larger effect on the %C_{37:4} than salinity.
104 Further complicating the use of long chain alkenones for SST reconstructions, Ono et al.
105 (2012) established using culture experiments that salinity had an effect on alkenone
106 unsaturation ratios at 20°C, but not at 15°C.

107 In addition to looking at alkenone amounts and distributions to infer salinity changes,
108 culture studies have shown the hydrogen isotopic composition (δD) of long chain alkenones
109 strongly depends on salinity as well (Schouten et al., 2005). M'boule et al. (2014) confirmed
110 in culture experiments involving both *I. galbana* (a coastal species) and *E. huxleyi* (an open
111 ocean species) that a strong linear relationship exists between δD and salinity, suggesting that
112 δD of alkenones might indeed be used to reconstruct relative shifts in paleosalinity. However,
113 coastal species, such as *I. galbana* and *Chrysothila lamellosa*, have been observed to
114 fractionate almost 100‰ less against deuterium than more open marine species, such as *E.*
115 *huleyi* and *Gephyrocapsa oceanica*, in culture (Schouten et al., 2005; Chivall et al., 2014;
116 M'boule et al., 2014). The δD of sedimentary alkenones might therefore also be indicative of
117 specific alkenone producing haptophytes.

118 The present day Baltic Sea has a large range in salinities (~3.5-32 PSU), with fresher
119 water in the northeastern part of the basin (including the Gulf of Bothnia and Gulf of Finland)
120 and saltier water closer to the connection to the North Sea (ICES-CIEM, n.d.) making it an
121 interesting site to study present-day salinity effects on alkenone production. Schulz et al.
122 (2000) demonstrated that alkenone unsaturation ratios in surface sediments of the Baltic Sea

123 have a low correlation to mean annual SST and instead primarily reflect salinity changes. The
124 authors postulate that lower salinity in parts of the basin causes salinity stress induced
125 changes in alkenone biosynthesis. This, together with the production of alkenones by
126 haptophytes adapted to lower salinities, results in distinct alkenone patterns with lower
127 salinity regions of the basin having patterns more characteristic of freshwater haptophytes or a
128 mixture of freshwater and marine haptophytes, and saltier regions having distributions that
129 resemble more marine haptophyte derived alkenones. Blanz et al. (2005) also reported that in
130 the Baltic Sea salinity-induced stress on *E. huxleyi* could alter the biosynthesis of alkenones,
131 thus affecting the use of the alkenone unsaturation ratios as a proxy for SSTs. Also, the
132 absence of C₃₈ methyl ketones observed in lower salinity water masses in the Baltic Sea has
133 been observed in Chinese Lakes as well (Song et al., 2016).

134 Here we determine how alkenone distributions and concentrations, along with the δD of
135 alkenones, varied with past changes in salinity in the Baltic Sea over the Holocene. Not only
136 does salinity vary regionally over the Baltic Sea basin today, but the Baltic Sea also has had a
137 complex salinity history since the last deglaciation and has gone through two fresh water and
138 two brackish water stages (see Section 2.1 for more details). In this study we examined a
139 Holocene record from the Arkona Basin to determine if changes in alkenone amounts and
140 distribution patterns that exist today and correlate with salinity around the basin also existed
141 in the past and co-varied with historical salinity changes.

142

143 **2. Methods**

144 *2.1. Historical setting of the Baltic Sea and description of the study site*

145 The Baltic Sea (Fig. 1) is the world's largest brackish body of water with an area of about
146 377,000 km² that is partitioned into multiple sub-basins. The Baltic is almost entirely enclosed

147 by land with a large freshwater contribution (including precipitation) of $660 \text{ km}^3 \text{ yr}^{-1}$ from a
148 drainage basin that is 1.6 million km^2 (Björck, 1995). An inflow of $475 \text{ km}^3 \text{ yr}^{-1}$ of saltwater
149 pours in through the only connection to the North Sea, the narrow Straits of Denmark
150 (Tikkanen and Oksanen, 2002). The Baltic Sea is a fairly shallow basin and on average only
151 about 54 m deep. The salinity varies greatly in the Baltic Sea ranging from ~ 3.5 PSU in the
152 north to ~ 8 PSU in the Baltic proper and ~ 32 PSU in the region where the Baltic connects to
153 the North Sea (ICES-CIEM, n.d.). A permanent halocline exists at about 13-15 m depth,
154 separating a relatively fresh surface and saline bottom waters.

155 The development of the Baltic Sea since the last deglaciation has been the focus of many
156 studies in the last decades (Winterhalter, 1992; Björck, 1995; Jensen, 1995, 1999; Andrén et
157 al., 2000). Reasons for such intense scientific interest include the shifting bathymetry,
158 dynamic hydrology and the resulting fluctuating salinity of the Baltic Sea over the Holocene
159 as the basin went through several different phases. Following deglaciation and before its
160 present state, the Baltic Sea transformed from the freshwater Baltic Ice Lake (c. 12.6-10.3 ka
161 BP) to the slightly brackish Yoldia Sea (c. 10.3-9.5 ka BP) into the freshwater Ancylus Lake
162 (c. 9.5-8.0 ka BP) and then into the brackish Littorina Sea (c. 8.0-3.0 kyr BP) and
163 subsequently into the Post-Littorina Sea / modern Baltic Sea (Winterhalter, 1992; Björck,
164 1995; Andrén et al., 2000). The Baltic Ice Lake formed as large areas of the southern Baltic
165 basin became ice free. Rapid deglaciation resulted in the uplift of the seabed, bringing the
166 connection of the basin with the North Sea above sea level and causing a large influx of fresh
167 melt-water into the system (Björck, 1995). A climatic cooling resulted in less meltwater and
168 the gradually receding ice sheet allowed drainage of the Baltic Ice Lake to occur, lowering the
169 water level and resulting in a short period of seawater ingressions, which characterized the
170 very slightly brackish Yoldia Sea (Björck et al., 1995; Jensen, 1995). Continued isostatic
171 rebound caused the basin to be once again cut off from the ocean and resulted in the Ancylus

172 Lake (Jensen et al., 1999). Then, at around 8,000 years ago, eustatic sea level rise re-opened
173 the connection with the North Sea through the Danish Straits allowing salt water to flow into
174 the Ancylus Lake and transforming it into the brackish Littorina Sea (Winterhalter, 1992).
175 The Ancylus Lake/Littorina Sea transition is a complex period characterized by different
176 phases of brackish-water pulses, initially weak and eventually resulting in fully established
177 brackish conditions (15-20‰ in the Baltic proper; Hyvärinen et al., 1988) only after ~2,000
178 years (Andren et al., 2000). The Littorina Sea phase, which lasted from ~8,000-3,000 BP, is
179 characterized by a warmer climate and thought to reflect the most marine-like conditions in
180 the Baltic Sea since deglaciation (Andren et al., 2000). The Post-Littorina Sea/modern Baltic
181 Sea are a continuation of the Littorina Sea, but with a salinity thought to be almost half (7-8‰
182 in the Baltic proper; Hyvärinen et al., 1988) that of the Littorina Sea (Punning et al., 1988).

183 *2.2. Sampling*

184 Two sediment cores were retrieved from the Arkona Basin, which extends from the
185 Bornholm Basin to the Danish Isles of Falster and Zealand (Fig. 1; Table 1). This basin
186 represents a boundary between the Straits of Denmark, where high salinity water flows in, and
187 the lower salinity Baltic Sea basin. The total discharge of brackish water from the basin is on
188 the order of 950 km³/yr (Björck, 1995). Both sediment cores were 12 m long and collected
189 using a gravity corer on the R/V “Maria S. Merian” in April of 2006. Sediment core 318310
190 was recovered at 46 m water depth at 54°50.34’N and 13°32.03’E and core 318340 was
191 collected nearby at 54°54.77’N and 13°41.44’E at 47 m water depth.

192 Two surface sediment samples from the Skagerrak obtained using a multi-corer
193 provided a marine end member for comparison with our Baltic Sea sediment core samples.
194 The surface sediment samples were collected during R/V “Elisabeth Mann-Borgese” cruise
195 EMB046 in May 2013. The sampling site for EMB046-10 was positioned at 57°49.74’N and

196 07°17.66'E from 457 m water depth. Site EMB046-20 was situated a bit to the east of
197 EMB046-10 at 58°31.60'N and 09°29.09'E from 532 m water depth.

198 *2.3. Loss on ignition (LOI)*

199 The LOI was determined by ashing freeze-dried sediments at 550°C for 3 h. The
200 resulting mass difference was then calculated in wt.%. Previously, it was demonstrated that
201 LOI provides an accurate estimate of the total organic carbon content of the sediments in the
202 Baltic Sea (Leipe et al., 2011). In order to obtain estimates for the total organic carbon (TOC;
203 %) content to normalize the concentration of ketones in the sediments, LOI values were
204 divided by 2.5 (i.e. assuming that the organic matter contains on average 40% C; Dean, 1974)

205 *2.4. X-ray fluorescence (XRF) core scanning*

206 XRF elemental scanning of sediment cores 318310 and 318340 was performed with
207 an Avaatech XRF scanner (Avaatech, n.d.) at a resolution of 0.5 cm.

208 *2.5. Correlation of sediment cores and age model*

209 Sediment cores 318310 and 318340 were correlated to each other on the basis of LOI
210 and XRF-Ca records (Fig. 2). The transition of the Ancyclus Lake phase to the Littorina Sea
211 phase is marked by a substantial increase in the TOC content, coinciding with color change of
212 the sediment (e.g. Moros et al., 2002; Rößler et al., 2011). Just after the large increase in TOC
213 (here reflected in the LOI record), there is a maximum in the carbonate content (here reflected
214 in the maximum in the elemental XRF- Ca record) (Fig. 2), which is caused by the occurrence
215 and preservation of benthic foraminifera (Moros et al., 2002; Rößler et al., 2011). The
216 Ancyclus Lake regression is also characterized by a clear peak in the LOI (TC) records, which
217 can be used for correlation purposes (Fig. 2). The transitions, Baltic Ice Lake/ Yoldia Sea and
218 Yoldia Sea/Ancyclus Lake are revealed by marked changes in the elemental XRF-Ca

219 (carbonate) and bulk density records (Fig. 2; see Moros et al., 2002), and by basin-wide
220 traceable sandy layers (Moros et al., 2002).

221 The age model for sediment core 318310 is based on a previous AMS¹⁴C date (7.2 cal
222 kyr BP) on *Mytilus edulis* close to the base of the Littorina phase (Rößler et al., 2011) and five
223 additional dates on mollusc shells (Fig. 2). The age model of the section of sediment core
224 318340 that was studied (400-840 cm) is based on the carbonate maximum at 380 cm (7.2 cal
225 kyr BP; Moros et al., 2002; Rößler et al., 2011). The start of the Ancylus Lake/Littorina Sea
226 transitional phase at 7.7 cal. kyr BP (unpublished results) is revealed by the increase in the
227 LOI record at 485 cm, and the Ancylus Lake regression at 10.2 cal kyr BP is denoted by the
228 sharp peak in the LOI record (sandy layer; Moros et al., 2002) at 600 cm. The boundary
229 between the Yoldia Sea phase and the Ancylus Lake phase (10.6 cal kyr BP; Moros et al.,
230 2002) at 768 cm, and the boundary between the Baltic Ice Sea and Yoldia Sea phases (11.6
231 cal. kyr BP; Moros et al., 2002) at 895 cm.

232 2.6. Lipid extraction and analysis

233 The sediments were freeze dried and ground and homogenized by mortar and pestle
234 for extraction. In general, 1-3 g of sediment was extracted using a DionexTM accelerated
235 solvent extractor with dichloromethane/methanol (9:1; v/v) as extraction solvent. The total
236 lipid extract was dried over a Na₂SO₄ column and then separated into three fractions using
237 Al₂O₃ column chromatography: apolar (eluted with 9:1 v/v hexane/DCM), ketone (1:1 v/v
238 hexane/DCM), and polar (1:1 v/v DCM/MeOH) fractions. The ketone fraction was then base
239 hydrolyzed by refluxing the dry fraction in a 1 N KOH in MeOH solution for 1 h after which
240 the pH was adjusted using a 2 N HCL/MeOH solution. DCM was added and the solution was
241 washed twice with DCM. The DCM layers were removed and combined to be dried over a
242 Na₂SO₄ column. After the addition of a nonadecan-10-one internal standard, the alkenone

243 fraction was analyzed using gas chromatography (GC) with an Agilent 6890 instrument
244 equipped with an Agilent CP-Sil 5 CB column (50 m x 0.32 i.d.; 0.12 μm film thickness) and
245 a temperature program from 70°C increasing at 20°C/min to 200°C and then at 3°C/min to
246 320°C where it remained stable for 44 min. Alkenones were identified by GC-mass
247 spectrometry (GC-MS), including the $\text{C}_{36:2}$ alkenone, using an Agilent 7890A GC instrument
248 equipped with a Agilent 5975C VL mass selective detector (MSD) and by comparing relative
249 retention times with those of known alkenones of a culture of *E. huxleyi*. Peak areas were
250 used to calculate alkenone unsaturation indices and alkenone concentrations were determined
251 based on peak responses relative to the nonadecan-10-one internal standard.

252 2.7. Compound specific hydrogen isotope compositions

253 Alkenone hydrogen isotope analyses were carried out on a subset of the samples, i.e.
254 those containing sufficient amounts of alkenones, on a Thermo Scientific DELTA⁺ xl
255 GC/TC/irMS. The temperature conditions of the GC increased from 70 to 145°C at 20°C min⁻¹
256 ¹, then at 8°C min⁻¹ to 200°C and to 320°C at 4°C min⁻¹, at which it was held isothermal for 20
257 min using an Agilent CP Sil-5 column (25 m x 0.32 mm) with a film thickness of 0.4 μm and
258 helium as carrier gas at 1 ml min⁻¹ (constant flow). The high temperature conversion reactor
259 was set at a temperature of 1425°C. The H_3^+ correction factor was determined daily and was
260 constant at 5.6±0.2 before and 3.8±0.1 after a scheduled power outage and retuning of the
261 irm. A set of standard n-alkanes with known isotopic composition (Mixture B prepared by
262 Arndt Schimmelmann, University of Indiana) was analyzed daily prior to analyzing samples
263 in order to monitor the system performance. Samples were only analyzed when the alkanes in
264 Mix B had an average deviation from their off-line determined value of <5‰. Squalane was
265 co-injected as an internal standard with each sample to monitor the accuracy of the alkenone
266 isotope values. The δD of long chain C_{37} alkenones were measured as the combined C_{37}
267 alkenones ($\delta\text{D}_{\text{alkenone}}$) (van der Meer et al., 2013) and the same applies to the C_{38} alkenones.

268 The squalane standard yielded an average $\delta D_{\text{alkenone}}$ value of -160.7 ± 2.7 , which is stable but
269 relatively enriched in D compared to its offline determined δD value of -170 ‰, potentially
270 due to co-eluting compounds in this sample set.

271 2.8. Calculation of alkenone based proxies

272 $\%C_{37:4}$ is the contribution of the tetra-unsaturated 37-carbon methyl alkenone ($C_{37:4}$) to
273 total C_{37} alkenone concentrations and calculated according to Rosell-Melé (1998):

$$274 \quad \%C_{37:4} = C_{37:4} / (C_{37:2} + C_{37:3} + C_{37:4}) \times 100 \quad (1)$$

275 The U_{37}^K index represents the relative abundance of the diunsaturated ($C_{37:2}$), triunsaturated
276 ($C_{37:3}$), and tetraunsaturated ($C_{37:4}$) methyl ketones (Brassell et al., 1986). Later, the
277 tetraunsaturated methyl ketone ($C_{37:4}$) was removed from the equation because this compound
278 was rarely found in open-sea sediments or suspended water column particles and the equation
279 was modified by Prahl and Wakeham (1987):

$$280 \quad U_{37}^K = C_{37:2} / (C_{37:2} + C_{37:3}) \quad (2)$$

281 2.9. Statistical analysis

282 Utilizing the R software package for statistical analysis, principle component analysis
283 (PCA) based on the correlation matrix was executed on the fractional abundances of the eight
284 alkenones quantified in the sediments studied. Four sediment samples from sediment core
285 318340 with no alkenones present were omitted from the PCA.

286 3. Results

287 3.1. Phases of the Baltic Sea covered in the Arkona Basin record

288 The XRF (Ca) and LOI (TC) data were used to distinguish different phases captured
289 by each sediment core in this study (Fig. 2) and to correlate the two sediment cores (see

290 methods). The sedimentary record for sediment core 318310 covers the upper section of the
291 freshwater Ancylus Lake stage starting at 10.2 cal kyr BP (642.5 cm), but mostly spans the
292 brackish phase of the basin beginning from 7.1 cal kyr BP (600-20 cm) (Fig. 2a). From
293 sediment core 318310 we studied eight sediment samples representing the brackish phase
294 including the Littorina Sea and Post-Littorina Sea / modern Baltic Sea stage and two samples
295 representing the Ancylus Lake stage (Fig. 2a; Table 1). To obtain more information on
296 alkenone occurrence and distribution during the Ancylus Lake stage, we also studied samples
297 from another sediment core. This core (318340) includes the complete Yoldia Sea stage (11.6-
298 10.6 cal kyr BP; 847.5-780.5 cm), the Ancylus Lake stage (10.6-7.7 cal kyr BP; 750.5-500.5
299 cm), and the Littorina Sea / Post Littorina Sea stage (7.2 -0 cal kyr BP; 400.5-0 cm) (Fig. 2b).
300 We analyzed 14 sediment samples from this core spanning depths 840.5-400.5 cm (Fig. 2b;
301 Table 1).

302 *3.2. Alkenone concentrations and distributions*

303 Total alkenone concentrations were generally higher (i.e. 32 ± 45 $\mu\text{g/g C}$;
304 average \pm standard deviation) in the brackish portion of the Arkona Basin record than for the
305 freshwater portion of the record (11 ± 17 $\mu\text{g/g C}$; Table 1). In the latter case, there were also
306 sediment horizons that did not contain detectable concentrations of alkenones. In the
307 sediments of the Yoldia Sea phase no alkenones were detected (Table 1). Fig. 3 shows some
308 typical alkenone distributions from sediment core 318310. Alkenones are comprised of the
309 more common $\text{C}_{37:2}$, $\text{C}_{37:3}$, and $\text{C}_{37:4}$ methyl (Me) ketones, $\text{C}_{38:2}$ and $\text{C}_{38:3}$ methyl (Me) and
310 ethyl (Et) ketones, and the uncommon $\text{C}_{36:2}$ Me ketone. This latter alkenone has not been
311 previously reported in sediments of the Baltic Sea. It is especially relatively abundant in
312 sediments deposited during the Littorina Sea period. Skagerrak surface sediments (Fig. 1)
313 were analyzed as a marine end member for comparison with the results obtained from the
314 Arkona Basin record. We did not detect the presence of the $\text{C}_{36:2}$ alkenone in the Skagerrak

315 sediments (Fig. 3a; Table 1). In sediment core 318310 a large difference in the relative
316 abundance of C₃₆, C₃₇ and C₃₈ alkenones is observed from 600 cm depth (c. 7.1 cal kyr BP;
317 Fig. 3d), which is close to the Ancylus Lake/Littorina Sea transitional phase, to more recent
318 sediments from the brackish phase of the Baltic Sea, i.e. at 100 cm (0.9 cal kyr, BP) and 50
319 cm (0.4 cal kyr BP) depth (Fig. 3b-c). For the Skagerrak surface sediments the alkenone
320 distribution is representative of a more open ocean setting (Fig. 3a). The alkenone distribution
321 at 50 cm depth (Fig. 3b) is more similar to that of the Skagerrak sample than any of the other
322 alkenone distributions shown (Fig. 3d), however, there are still a few differences between the
323 two, such as the absence of the C_{36:2} alkenone and the lower relative abundance of C_{37:4} Me in
324 the Skagerrak sediments.

325 For a statistical evaluation of alkenone distribution changes, PCA was performed on
326 the distributions of C₃₆, C₃₇ and C₃₈ alkenones in the different sediments studied. Most of the
327 variation is explained by principle component 1 (PC1; expressing 41% of the variance), which
328 is related to the degree of unsaturation of the alkenones with the most unsaturated alkenones
329 scoring negatively on PC1 (Fig. 4a). This is confirmed by the good correlation ($r^2 = 0.86$) of
330 the score on PC1 with U_{37}^K (Fig. 4e). The variation in PC2 (27%) appears to be mostly
331 explained by the fractional abundance of the C_{36:2} alkenone, which scores negatively on PC2
332 (Fig. 4a). Indeed, the score on PC2 significantly ($r^2 = 0.77$) negatively correlates with the
333 fractional abundance of the C_{36:2} alkenone (Fig. 4f). PC3 explains 18% of the variance with
334 the C₃₈ Et ketones scoring negatively on PC3 (Fig. 4c). PC3 correlates significantly ($r^2 = 0.77$)
335 negatively with the summed fractional abundance of the C_{38:3} and C_{38:2} Et ketones (Fig. 4g).

336 Most sediments score between -1 and +1 on PC2, however, the Skagerrak sediments
337 plot more positively (ca. 2.0) and sediments from the core 318310 from the Littorina Sea
338 phase (sediment core depths 400, 500 and 600 cm) plot more negatively on PC2 (ca. -3.2)
339 (Fig. 4b). Fig. 5a shows the scores of PC1-3 plotted as a function of age. This reveals that the

340 score on PC1 is mostly negative for sediments older than 7.2 cal kyr BP and is mostly positive
341 during the more recent phases of the Baltic Sea (after 7.2 cal kyr BP) (Fig. 5a). The score on
342 PC2 consistently plots positively throughout the combined record from the Arkona Basin
343 except for the sediment depths that correspond to the Littorina Sea phase (sediment core
344 depths 400-600 cm from core 318310, which spans 7.1-3.7 cal kyr BP) and the end of the
345 Ancylus Lake phase (sediment core depth 400.5 cm in core 318340, which spans 7.1-3.7 cal
346 kyr BP; Fig. 5a-b (Fig. 5a). Two other core 318340 samples that plot slightly negatively for
347 PC2 are depths 480.5 cm (7.7 cal kyr BP) and 750.5 cm (10.6 cal kyr BP) (Fig. 5a). PC3
348 scores mostly between -1 and 1 throughout the sediment record and for the Skagerrak
349 samples, however, some samples that fall within the Ancylus Lake phase plot outside of this
350 range as does sediment sample 100 cm from record 318310 (0.9 cal kyr BP; Figs. 4d and 5a).

351

352 3.3. δD of alkenones

353 We also determined δD values of alkenones on a subset of the samples from sediment
354 core 318310 (Table 2), which can be an indicator of environmental conditions, mainly salinity
355 and potentially haptophyte species composition (Schouten et al., 2005; van der Meer et al.,
356 2008, 2015; Chivall et al., 2014; M'boule et al., 2014). The surface sediment samples from
357 the Skagerrak have similar δD values for the C_{37} and C_{38} alkenones that fall between -175 and
358 -185‰ (Fig. 6; Table 2). In the Arkona Basin the C_{37} and C_{38} alkenones have lower δD values
359 during the more recent brackish phase going back to about 2.7 cal kyr BP, (-212.2±5.5‰)
360 (Fig. 6; Table 2). However, at the base of the Littorina Sea phase (7.1 cal kyr BP, 600 cm
361 sediment depth from sediment core 318310), the δD values for C_{37} (-182.4‰) and C_{38}
362 alkenones (-170.3‰) are much higher and, in contrast to the other samples, the C_{37} are more
363 depleted in D than the C_{38} alkenones. The obtained δD values of the $C_{36.2}$ alkenone deposited

364 during the brackish portion of the record in the Arkona Basin are enriched in D relative to the
365 C₃₇ and C₃₈ alkenones from the same samples, but similar to those of the C₃₇ and C₃₈
366 alkenones encountered in the modern day Skagerrak (-169.3±3.0‰). Just after the Ancyclus
367 Lake/Littorina Sea transition, the δD values of the C_{36:2} alkenone (-168.7‰) is similar to that
368 of the C₃₈ alkenones (-170.3‰; Fig. 6; Table 2).

369

370 **4. Discussion**

371 *4.1. Changes in sources of alkenones and its relation to changes in salinity*

372 The observed changes in the relative abundances of the different alkenones through
373 time may be a direct response of alkenone biosynthesis to changing environmental conditions
374 of the Baltic Sea over the Holocene, or alternatively, the changing conditions could result in
375 changing species composition leading to different alkenone distributions. There are many
376 characteristics of alkenones that have been linked to haptophyte species composition and/or
377 environmental conditions. The most important are:

378 (i) The degree of unsaturation of alkenones is commonly interpreted to be
379 predominantly dependent on growth temperature (Brassell et al., 1986; Prahl and Wakeham,
380 1987).

381 (ii) The relative abundance of the C_{37:4} alkenone is generally higher in coastal
382 haptophytes that thrive at lower salinities and this predominance is even more extreme in
383 freshwater systems (Rosell-Mele, 1998; Schulz et al., 2000; Blanz et al., 2005; Liu et al.,
384 2008, 2011).

385 (iii) The ratio of C₃₇/C₃₈ alkenones might be indicative of haptophyte species since
386 different C₃₇/C₃₈ values were observed for different haptophytes with coastal haptophytes

387 generally showing higher ratios compared to more open ocean species (Prah1 et al., 1988;
388 Conte et al., 1998; Schulz et al., 2000). However, it has also been shown that environmental
389 conditions, e.g. temperature, also affect the C₃₇/C₃₈ ratio (Conte et al., 1998; Sun et al., 2007).

390 (iv) The presence of the uncommon C_{36:2} alkenone, which only has been reported in
391 the Black Sea (Xu et al., 2001; Prah1 et al., 2006), Japan Sea (Fujine et al., 2006), and in an
392 estuary in Florida (Van Soelen et al., 2014). Previous studies suggested it to be an indicator of
393 brackish conditions (Xu et al., 2001; Fujine et al., 2006) and more recently, Coolen et al.
394 (2009) proposed its biological origin in the Black Sea is likely a strain of low salinity-adapted
395 *E. huxleyi*.

396 (v) The δD of alkenones, the values of which are characteristic of certain types of
397 haptophytes, but can also change with changing environmental conditions. Coastal
398 haptophytes tend to fractionate less than more open marine haptophytes (Schouten et al.,
399 2005; Chivall et al., 2014; M'boule et al., 2014), therefore, δD values can aid in assigning
400 biological sources of sedimentary alkenones. However, hydrogen isotope fractionation also
401 depends on environmental factors such as salinity, light intensity and growth rate (Schouten et
402 al., 2005; Prah1 et al., 2006; van der Meer et al., 2008, 2015; Wolhowe et al., 2015).

403 Some of these parameters were used to assign potential biological sources of the Baltic
404 Sea sedimentary alkenones. To this end, the Arkona Basin data was compared with that from
405 surface sediments of the Skagerrak (Figs. 4 and 6). Marine haptophytes, such as *E. huxleyi*,
406 living at higher salinities and in more open ocean settings (like the Skagerrak) with a salinity
407 of approximately 34 PSU (Danielssen et al., 1996) will fractionate at approximately 190‰
408 against D. Using a δD of Skagerrak water of ca. 0‰ (Frohlich et al., 1988) the δD values for
409 the C₃₇ and C₃₈ alkenones are predicted to be ca. -190‰ (Englebrecht and Sachs, 2005;
410 Schouten et al., 2005; M'boule et al., 2014). The δD value of the C₃₇ and C₃₈ alkenones in the

411 Skagerrak surface sediments is $-180\pm 5\text{‰}$ (Fig. 6; Table 2), indicating the haptophyte species
412 in this region are predominantly of the marine type, most likely derived from *E. huxleyi*.

413 The alkenones in the sedimentary record of the Arkona Basin up to ca. 2.7 cal kyr BP
414 have a distribution that is quite similar to that observed in Skagerrak surface sediments (Figs.
415 3a-c), which is typical of a marine haptophyte such as *E. huxleyi*. The low $\%C_{37:4}$ during this
416 time ($3.1\pm 2.3\%$) would also suggest that these alkenones are derived from marine type
417 haptophytes (i.e. *E. huxleyi*) (Fig. 5d). However, the C_{37} and C_{38} alkenones have substantially
418 lower δD values ($-212\pm 6\text{‰}$) than found in the Skagerrak surface sediments for the alkenones
419 ($-180\pm 5\text{‰}$; Fig. 6; Table 2). There are two main factors to consider. Firstly, the present-day
420 δD of surface waters in the Arkona Basin is ca. -40‰ averaged over the photic zone (Frohlich
421 et al., 1988), i.e. 40‰ depleted relative to the Skagerrak waters. This will shift the δD values
422 of alkenones to substantially lower values (e.g., Englebrecht and Sachs, 2005). Secondly,
423 culture studies have shown that hydrogen isotope fractionation is dependent on salinity,
424 among other factors, with increased fractionation at lower salinities (e.g. M'boule et al.,
425 2014). The present-day salinity of surface waters of the Arkona Basin is ~ 10 PSU (ICES-
426 CIEM, n.d.). If *E. huxleyi* would be able to grow at these low salinities, the alkenone δD value
427 is estimated at ca. -270‰ , which is substantially lower than the measured values for the C_{37}
428 and C_{38} alkenones ($-212\pm 6\text{‰}$). This value was arrived upon by extrapolating the isotope
429 fractionation (α)-salinity relationship to these low salinities (M'boule et al., 2014), and using
430 the δD value for surface waters of -40‰ over the photic zone (Frohlich et al., 1988).
431 Consequently, this indicates that an *E. huxleyi* only origin for the C_{37} and C_{38} alkenones in the
432 sedimentary record of the Arkona basin up to ca. 2.7 cal kyr BP, is unlikely. Haptophyte
433 species adapted to lower salinities, such as *I. galbana* or *C. lamellosa*, fractionate less against
434 D (Chivall et al., 2014; M'Boule et al., 2014), and the alkenones produced will have a less
435 negative δD value. For *I. galbana* (M'boule et al., 2014) a δD value of alkenones of ca. -

436 180‰ can be estimated using a salinity of 10 PSU the δD of surface waters of -40. This value
437 is higher than the values observed for the C_{37} and C_{38} alkenones in the Arkona Basin up to ca.
438 2.7 cal kyr BP (i.e. between -205 and -220‰). This suggests that these sedimentary alkenones
439 represent a mixture of alkenones produced by low salinity adapted haptophytes such as *I.*
440 *galbana* and higher salinity adapted haptophytes such as *E. huxleyi*, with a more substantial
441 contribution from the low salinity adapted haptophytes.

442 The $C_{36:2}$ alkenone was detected in the Arkona Basin sediments, but not in the
443 Skagerrak surface sediments (Fig. 3; Table 1). This supports the premise that the $C_{36:2}$
444 alkenone is exclusively produced by a low-salinity adapted haptophyte (Coolen et al., 2009).
445 PCA revealed that the fractional abundance of the $C_{36:2}$ alkenone is an important factor in the
446 changing alkenone distributions in the Baltic Sea (Figs. 4a and f); i.e. PC2, explaining 27% of
447 the total variance, is predominantly determined by the fractional abundance of the $C_{36:2}$
448 alkenone (Fig. 4a). In the sedimentary record of the Arkona Basin up to ca. 2.7 cal kyr BP, the
449 fractional abundance of the $C_{36:2}$ alkenone amounts to 0.10 ± 0.03 (Figs. 5c; Table 1). From
450 7.1-3.7 cal kyr BP in the sediment record the fractional abundance of the $C_{36:2}$ alkenone
451 increases to 0.51 ± 0.11 and it dominates the alkenone distribution (Figs. 3d and 5c; Table 1).
452 For the entire period of 7.1-0.1 cal kyr BP the δD values for the $C_{36:2}$ alkenone show only
453 minor variation and are similar to the δD values for the C_{37} and C_{38} alkenones from the
454 modern day Skagerrak (-170 ± 3 ‰; Fig. 6; Table 2). However, for most of the record the δD
455 value of the $C_{36:2}$ alkenone is significantly higher than those of the C_{37} and C_{38} alkenones.
456 Since the δD value of the $C_{36:2}$ alkenone is close to that (-180 ‰) calculated for *I. galbana*
457 using a salinity of 10 PSU and a δD of surface waters of -40‰ (see above) this suggests that it
458 is derived from a single low-salinity adapted haptophyte species. Previous studies (Coolen et
459 al., 2009; Van Soelen et al., 2014) have also reported a substantial offset in δD values for C_{37}
460 and $C_{36:2}$ alkenones with that of the $C_{36:2}$ alkenone being significantly higher. Van Soelen et al.

461 (2014) concluded that the offset in δD values for C_{37} and $C_{36:2}$ alkenones found in an estuary
462 in Florida is evidence that different haptophytes, yet still unknown, are producing the $C_{36:2}$
463 alkenone. Interestingly, close to the Ancyclus Lake/Littorina Sea transition (7.1 cal kyr BP,
464 600 cm sediment depth from core 318310), which falls within the period characterized by the
465 high fractional abundance of the $C_{36:2}$ alkenone, the δD values for C_{37} (-182.4‰) and C_{38} (-
466 170.3‰) alkenones are much higher than in the other Arkona Basin samples and similar to
467 the δD values of the $C_{36:2}$ alkenone (Fig. 6; Table 2). This suggests a similar origin for most of
468 the C_{36} , C_{37} and C_{38} alkenones at this time, most likely a low salinity adapted haptophyte
469 species. This is strongly supported by the deviating alkenone distribution at this time (Fig. 3d)
470 dominated by the $C_{36:2}$ alkenone. The observed trends in δD values of alkenones over the
471 period between 7.1 and 0.1 cal kyr BP, thus, corroborate the idea that during this period in the
472 Baltic Sea there is more than one alkenone producing haptophyte species.

473 From circa 7.1-3.7 cal kyr BP, during the Littorina Sea phase in the Baltic Sea, the
474 $C_{36:2}$ ratio is highest demonstrating the greatest contribution from these low-salinity adapted
475 haptophytes and the % $C_{37:4}$ is more variable during this period ranging from 0.1-13.6%. This
476 suggests mutable input from non-marine type haptophytes and therefore potentially
477 fluctuating salinities (Fig. 5d; Table 2). The enrichment in the δD of the C_{37} and C_{38} alkenones
478 corroborates the contribution from non-marine haptophytes as well (Fig 6). Why the % $C_{37:4}$
479 and the fractional abundance of the $C_{36:2}$ alkenone is higher and the C_{37} and C_{38} alkenones are
480 more enriched in D during the Littorina Sea phase than after is not clear since they are both
481 brackish water periods. Possibly this is related to the period after the Ancyclus Lake/Littorina
482 Sea transition being a time of not only low, but also variable salinity. Perhaps the haptophytes
483 producing the $C_{36:2}$ alkenone had a competitive advantage over other haptophytes at this time
484 because they were better adapted to changing salinities, or alternatively, certain haptophyte
485 species biosynthesize this compound in response to changing salinities or marine haptophytes

486 brought in from the North Sea were not yet established. These possibilities suggest that
487 variable salinity was a characteristic of the Littorina Sea phase.

488 Prior to 7.1 cal kyr BP in the Arkona Basin sediment record we do not have δD values
489 of alkenones to report, however, some remarkable changes in the alkenone distributions are
490 observed. Firstly, the $U^{K'}_{37}$ is lower prior to the Ancyclus Lake/Littorina Sea transition (Fig.
491 5e) potentially due to a change in the composition of the haptophyte community as indicated
492 by the higher fractional abundance of the $C_{37:4}$ at this time (Fig. 5d; Table 1). Secondly, the
493 fractional abundance of the $C_{36:2}$ alkenone is relatively low from 10.7 cal kyr BP up to the
494 transition (0.02 ± 0.03 ; Fig. 5c; Table 1). Thirdly, during the transitional phases of this time
495 period, both the Yoldia Sea phase to Ancyclus Lake transition (c. 10.7-10.6 cal kyr BP) and at
496 the Ancyclus Lake/Littorina Sea transition (c. 7.3 cal kyr BP), the alkenone distributions are
497 dominated by C_{38} ethyl alkenones (i.e. a low score on PC3; Figs. 4c-d and i.e. summed
498 average fractional abundance of 0.55 ± 0.03 ; Fig. 5b; Table 1). The lower fractional abundance
499 of the $C_{36:2}$ alkenone during the Ancyclus Lake phase, (Fig. 5c; Table 1) suggests that most
500 likely a change in haptophyte species composition occurred related to salinity. Additionally,
501 the $C_{36:2}$ alkenone is absent in the Arkona Basin sedimentary record from 10.2-8.0 cal kyr BP
502 (Fig. 5c; Table 1). Since it is a potential indicator for the low salinity adapted, but not
503 freshwater haptophyte species, the presence of the $C_{36:2}$ alkenone prior to the Ancyclus Lake
504 phase ending suggests marine influxes had already begun in the basin at that time. A diatom
505 study by Witkowski et al. (2005) reported that the first brackish water inflows began just
506 before this time period, i.e. between 8.9-8.4 kcal yr BP. The presence of the $C_{36:2}$ alkenone
507 from 10.6-10.2 cal kyr BP aligns with the ending of the slightly brackish Yoldia Sea phase.
508 Lastly, the higher $\%C_{37:4}$ during the Ancyclus Lake phase verifies that there was an increase in
509 freshwater haptophytes during this time.

510 *5.2. Comparison with the Holocene alkenone record of the Black Sea*

511 A previous study of alkenones in the Black Sea (Coolen et al., 2009) reported similar
512 trends with respect to the fractional abundance of the C_{36:2} alkenone to those reported here for
513 the Baltic Sea. The Black Sea experienced a somewhat comparable geological history to the
514 Baltic Sea. In the early Holocene it was a freshwater lake until a connection was established
515 with the Aegean and Mediterranean Seas due to the global transgression allowing the influx
516 of more saline waters (Ryan et al., 1997). The permanent establishment of this connection is
517 dated at c. 7.2 cal kyr BP (Ryan et al., 1997; Ballard et al., 2000). The resultant increase in
518 salinity is reflected by the sedimentary sequence revealing a transition from banded clay with
519 graded sand and silt layers (Unit III) to sapropel mud (Unit II) (Ross et al., 1970). As the
520 influx of salty Mediterranean waters continued it caused an increase in the surface salinity of
521 the Black Sea allowing a massive growth of *E. huxleyi* (Jones and Gagnon, 1994) in the basin
522 c. 2.7 cal kyr BP, resulting in deposition of a coccolith ooze (Jones and Gagnon, 1994). The
523 abundance in *E. huxleyi* at this time has been attributed to a surface water salinity increasing
524 above 11 PSU and the base of Unit I is generally defined as the horizon that reveals the first
525 invasion of *E. huxleyi*, ca. 700 yr earlier (Fig. 7) (Arthur and Dean, 1998; Hay, 1988).

526 Since the salinity changes in the Baltic Sea and Black Sea occurred around the same
527 time (~7.2 cal kyr BP), we compared the relative abundance of the C_{36:2} alkenone from the
528 Baltic Sea directly to that in the Black Sea reported by Coolen et al. (2009) (Fig. 7a). In both
529 the Baltic Sea and Black Sea the fractional abundance of the C_{36:2} alkenone is rapidly
530 increasing to values of 40-70% just after the inflow of more saline waters started.
531 Subsequently, a period of sustained high fractional abundances follows in both basins up to
532 ca. 2.6 cal kyr BP. The higher resolution record of the Black Sea shows that the period
533 between 7.0-5.4 cal kyr BP is characterized by the highest values (up to 75%), followed by a
534 drop to a fractional abundance of ca. 25% for the period 5.0-2.6 cal kyr BP. This latter period
535 is interrupted by the horizon of the first invasion of *E. huxleyi* at 3.5 cal kyr BP when the

536 fractional abundance drops to 5%. For the Baltic Sea the fractional abundance of the C_{36:2}
537 alkenone is high throughout the 7.0-2.6 cal kyr BP period. In both basins the fractional
538 abundance of the C_{36:2} alkenone is substantially reduced in the most recent period (2.6-0.0 cal
539 kyr BP) although for the Baltic Sea it does not drop to the low values seen in the Black Sea
540 (i.e. 1%) and it increases towards the present day situation (Fig. 7a). In conclusion, we note a
541 quite similar behavior for the fractional abundance of the C_{36:2} alkenone in both enclosed
542 basins with limited connection to the open ocean. This may relate to a somewhat comparable
543 response to the global sea level transgression during the Holocene. For the Black Sea
544 substantial additional data is available for the interpretation of this trend and this may help, by
545 analogy, to provide a more detailed interpretation of the Baltic Sea record.

546 Coolen et al. (2006, 2009) provided through ancient DNA analysis clues on the
547 biological origin of the sedimentary alkenone in the Black Sea. The most extensive record
548 comes from a site in the western Black Sea. It reveals that during deposition of the base of
549 Unit II *Isochrysis*-related haptophytes thrived (Fig. 7c). This fits with the time of the newly
550 established connection with the Mediterranean since these type of haptophytes are adapted to
551 low salinity. Subsequently, there is a short period (5.7-4.8 cal kyr BP) where Coolen et al.
552 (2009) detected both *Isochrysis*-related haptophytes and *E. huxleyi*, followed by a period
553 where only ancient DNA of *E. huxleyi* was found. When this information is combined with
554 the record of the fractional abundance of the C_{36:2} alkenone (Fig. 7a), it is evident that this
555 alkenone must have been produced by *Isochrysis*-related haptophytes since the period of
556 highest fractional abundance (up to 75%) falls in the period where only ancient DNA of
557 *Isochrysis*-related haptophytes is detected (Fig. 7). However, the C_{36:2} alkenone also occurs
558 (albeit at a substantially reduced fractional abundance) in more recent periods when only
559 ancient DNA of *E. huxleyi* is detected, suggesting that this haptophyte may also produce this
560 alkenone. However, this latter conclusion is at odds with the large difference (90-100%) in

561 δ D composition of the C_{36:2} and C₃₇ alkenones as reported by Giosan et al. (2012) for this
562 section, which indicates clearly distinct biological sources for these alkenones. In fact, when
563 the δ D record of the C_{36:2} alkenone is combined with the recent determination of the isotopic
564 fractionation factor α for *Isochrysis galbana* (M'boule et al., 2014) to estimate palaeosalinity
565 of the surface waters of the Black Sea over the Holocene, we obtain a record (Fig. 7c; blue
566 line) that is in good agreement with our general concept of the development of surface salinity
567 of the Black Sea. In the lowermost part of Unit II the estimated palaeosalinity is only a few
568 PSU, it subsequently rises to 15 PSU at the Unit I/II transition, reaches a maximum of ca. 26
569 PSU at 2.0 cal kyr BP and then declines to 17 PSU for the most recent period. These data are
570 in good agreement with salinity calculations (Fig. 7c) based on δ D data of C₃₇ alkenones in
571 cores from both the western and eastern Black Sea (van der Meer et al., 2008; Giosan et al.,
572 2012) in combination with the isotopic fractionation factor α for *E. huxleyi* (M'boule et al.,
573 2014). For the period where the fractional abundance of the C_{36:2} alkenone is still elevated (i.e.
574 up to 2.6 cal kyr BP) these estimations of paleosalinity are on the high end (except for the
575 horizon reflecting the first invasion of *E. huxleyi* in the Eastern Basin). This is most likely
576 caused by the fact that the C_{36:2} alkenone-producing haptophytes are also contributing D-
577 enriched C₃₇ alkenones to the total pool of C₃₇ alkenones, influencing the palaeosalinity
578 calculation that is based on a 100% origin from *E. huxleyi*. Hence, the δ D data of the C_{36:2}
579 alkenone in combination with the salinity calculations strongly suggest that the C_{36:2} alkenone
580 has been produced by an *Isochrysis*-related haptophyte and not by a lower salinity adapted
581 strain of *E. huxleyi* as suggested previously (Coolen et al., 2009). It remains unclear why
582 ancient DNA of this haptophyte is only detected for the period 7.4-4.8 cal kyr BP. However, it
583 is known that Denaturing Gradient Gel Electrophoresis (DGGE), the method used by Coolen
584 et al. (2009) to detect ancient DNA is only able to quantify the predominant DNA sequences.

585 Combining the fractional abundance record of the C_{36:2} alkenone (Fig. 7a) with the
586 palaeosalinity record (Fig. 7c) now makes it possible to determine the optimal salinity for the
587 *Isochrysis*-related haptophyte producing the C_{36:2} alkenone. In the Black Sea at salinities from
588 2-8 PSU, the C_{36:2} alkenone dominates the alkenone distribution. At a salinity of up to ca. 19
589 PSU the C_{36:2} alkenone can still contribute substantially (25%) and above this level it becomes
590 a minor alkenone. It is clear that salinity is not the only environmental control on the C_{36:2}
591 alkenone-producing haptophyte since when in recent times salinities drop to ca. 17 PSU, the
592 C_{36:2} alkenone still remains a minor alkenone (Fig. 7).

593 The C_{36:2} alkenone data of the Black Sea allow the interpretation of the C_{36:2} alkenone
594 record of the Baltic Sea in term of changes in salinity. This should be done cautiously since it
595 is clear that other environmental factors also may have an effect. Nevertheless, the sudden
596 increase of the fractional abundance of the C_{36:2} alkenone record at the Ancyclus Lake/Littorina
597 Sea transition is highly comparable to what happened in the Black Sea at the Unit III/II
598 transition and indicates an incursion of marine waters into the freshwater lakes most probably
599 by the worldwide sea level transgression, resulting in a modest increase in surface water
600 salinity to ca. 2 PSU. In the Baltic Sea the fractional abundance of the C_{36:2} alkenone remains
601 high until ca. 3.0 cal kyr BP, suggesting that the salinity of the surface waters of the Arkona
602 Basin increased at a lower rate than in the Black Sea. The lowest fractional abundance of the
603 C_{36:2} alkenone is recorded in the Arkona Basin at 0.9 cal kyr BP, suggesting that the salinity
604 was highest at that time, which corresponds to the medieval climate anomaly (MCA, which
605 occurred between 950-1,250 BP). This trend is similar to salinity records for the whole Baltic
606 Sea based on combined proxies and modelling (Gustafsson and Westman, 2002) although the
607 maximum salinity is thought to be earlier even when we correct for the different age models.
608 Generally, it is believed that the Littorina phase of the Baltic Sea was more saline than the
609 post-Littorina phase, however, other studies do not reveal this difference (Andren et al., 2000;

610 Westman and Sohlenius, 1999; Andrén et al, 2002; Witkowski et al., 2005) or show the
611 opposite (Emeis et al., 2003).

612

613 *5.3 Potential uses of alkenones as environmental indicators for SST*

614 The indices and ratios we have presented in this study all corroborate that a haptophyte
615 species composition change, most likely driven by a salinity shift, occurred during the Yoldia
616 Regression (10.6 cal kyr BP), the Ancylus Lake/Littorina Sea transition (7.7-7.2 cal kyr BP),
617 and at the MCA (0.9 cal kyr BP). The results also indicate that the haptophyte species
618 composition since 7.2 cal kyr BP in the Baltic Sea basin is a combination of marine (*E.*
619 *huxleyi* type) and low-salinity adapted haptophytes. This designates that higher salinity
620 conditions have prevailed since the Ancylus Lake/Littorina Sea transition.

621 To determine how shifts in haptophyte species composition in the Baltic Sea could
622 affect paleoclimate reconstructions using long chain alkenones, we examined the $U^{K'}_{37}$ index
623 over the Holocene. $U^{K'}_{37}$ values changed across the Ancylus Lake/Littorina Sea transition
624 with lower values (0.24 ± 0.04) during the Ancylus Lake phase and an increase in the $U^{K'}_{37}$
625 index after 7.2 cal kyr BP (0.42 ± 0.15 ; Fig. 5e; Table 2). This resulted in an increase in
626 average estimated SSTs based on the $U^{K'}_{37}$ index from $\sim 6^\circ\text{C}$ during the Ancylus Lake phase
627 to $\sim 13^\circ\text{C}$ during the brackish phase. We believe that variations in haptophyte community
628 composition resulting from fluctuating salinity is most likely responsible for this change in
629 $U^{K'}_{37}$ values and the corresponding unrealistic increase in SST over the Ancylus
630 Lake/Littorina Sea transition. The highest contribution of the $C_{36:2}$ alkenone occurred during
631 the Littorina Sea phase, which indicates salinity was relatively low at that time. The presence
632 of this alkenone even in the more recent phase of the Baltic Sea is evidence of the continued
633 contribution from low salinity adapted haptophytes, which are most likely complicating the

634 use of alkenone unsaturation ratios for SST reconstructions in this region. Schulz et al. (2000)
635 demonstrated in a study performed in the Baltic Sea that $U^{K'}_{37}$ varied regionally depending on
636 salinity and that higher salinity areas in the Baltic had higher $U^{K'}_{37}$ values and vice versa.
637 Since previous studies have also shown that alkenone distributions co-vary not only with
638 temperature changes, but also with salinity driven changes in haptophyte species composition
639 (Coolen et al., 2004, 2009) we cannot apply the $U^{K'}_{37}$ index for SST reconstructions in the
640 Baltic Sea basin over the Holocene.

641 Interestingly, we observed that during the brackish phase the alkenone distribution at
642 0.9 cal kyr BP (100 cm depth) is unique compared to the other sediment samples (Fig. 3) from
643 the brackish phase. This sediment horizon has the lowest contribution of the $C_{36:2}$ alkenone,
644 the lowest % $C_{37:4}$ and the highest fractional abundance of the C_{38} Et alkenone (Fig. 5b-d;
645 Tables 1-2), all indicating the increased presence of marine type haptophyte species and
646 therefore that more marine conditions prevailed in the Baltic Sea at this time. This sample
647 falls within the MCA, also known as the Medieval Warm Period. The lower contribution of
648 the $C_{37:3}$ alkenone compared with $C_{37:2}$ corroborate that warmer temperatures (Fig. 3c)
649 occurred during this time, although the minor contribution of *Isochrysis*-related haptophytes
650 do not allow absolute SST determination.

651

652 **Conclusions**

653 This research demonstrates the usefulness of alkenone distributions along with the δD of the
654 alkenones for paleosalinity studies in the Baltic Sea and other environments as well. Both
655 alkenone distributions and hydrogen isotopic composition indicate a shift in haptophyte
656 species composition in the Arkona Basin of the Baltic Sea from the Ancylus Lake to the
657 Littorina Sea phase, c. 7.2 cal kyr BP, from lacustrine to brackish type haptophytes,

658 corresponding to the incursion of marine waters that occurred in the Baltic Sea at that time as
659 a consequence of the global sea level rise. During the Littorina Sea Phase the fractional
660 abundance of the C_{36:2} alkenone remains high, suggesting that salinity did not rise above 8
661 PSU. From ca. 3.0 cal kyr BP onwards the fractional abundance of the C_{36:2} alkenone is lower,
662 suggesting a slightly higher salinity. During this phase there is a substantial offset in δD
663 values with the C_{36:2} alkenone substantially more enriched than the C₃₇ alkenones. The
664 presence of the C_{36:2} alkenone in the Baltic Sea as well as the δD record suggest it is produced
665 by a different species of haptophyte adapted to lower salinity conditions that is not
666 contributing much to the production of C₃₇ and C₃₈ alkenones. The contribution of alkenones
667 from lower salinity adapted species in the Baltic Sea hinders the use of the $U^{K'}_{37}$ index for
668 SST reconstructions.

669 **Acknowledgements**

670 We thank M. Verweij for help with the GC analysis and A. Mets for help with the GC-MS
671 analysis. This work was supported by the European Research Council under the European
672 Union's Seventh Framework Programme (FP7/2007-2013) / ERC grant agreement n°
673 [226600]. JSSD receives funding from the Netherlands Earth System Science Center
674 (NESSC) though a gravitation grant from the Dutch ministry for Education, Culture and
675 Science.

676 **References**

- 677 Andren, E., Andrén, T., Sohlenius, G., 2000. The Holocene history of the southwestern Baltic
678 Sea as reflected in a sediment core from the Bornholm Basin. *Boreas* 29, 233–250.
- 679 Arthur, M.A., Dean, W.E., 1998. Organic-matter production and preservation and evolution
680 of anoxia in the Holocene Black Sea. *Paleoceanography* 13, 395–411.

681 Ballard, R.D., Coleman, D.F., Rosenberg, G.D., 2000. Further evidence of abrupt Holocene
682 drowning of the Black Sea shelf. *Marine Geology* 170, 253–261.

683 Bendle, J., Rosell-Melé, A., Ziveri, P., 2005. Variability of unusual distributions of alkenones
684 in the surface waters of the Nordic seas. *Paleoceanography* 20, DOI:
685 10.1029/2004PA001025.

686 Björck, S., 1995. A review of the history of the Baltic Sea, 13.0-8.0 ka BP. *Quaternary*
687 *International* 27, 19–40.

688 Blanz, T., Emeis, K.C., Siegel, H., 2005. Controls on alkenone unsaturation ratios along the
689 salinity gradient between the open ocean and the Baltic Sea. *Geochimica et*
690 *Cosmochimica Acta* 69, 3589–3600.

691 Brassell, S.C., Eglinton, G., Marlowe, I.T., Pflaumann, U., Sarnthein, M., 1986. Molecular
692 stratigraphy: a new tool for climatic assessment. *Nature* 320, 129–133.

693 Chivall, D., M'Boule, D., Sinke-Schoen, D., Sinninghe Damsté, J.S., Schouten, S., van der
694 Meer, M.T., 2014. Impact of salinity and growth phase on alkenone distributions in
695 coastal haptophytes. *Organic Geochemistry* 67, 31–34.

696 Chu, G., Sun, Q., Li, S., Zheng, M., Jia, X., Lu, C., Liu, J., Liu, T., 2005. Long-chain
697 alkenone distributions and temperature dependence in lacustrine surface sediments from
698 China. *Geochimica et Cosmochimica Acta* 69, 4985–5003.

699 Conte, M.H., Thompson, A., Lesley, D., Harris, R.P., 1998. Genetic and physiological
700 influences on the alkenone / alkenoate versus growth temperature relationship in
701 *Emiliana huxleyi* and *Gephyrocapsa oceanica*. *Geochimica et Cosmochimica Acta* 62,
702 51–68.

703 Coolen, M.J., Muyzer, G., Rijpstra, W.I.C., Schouten, S., Volkman, J.K., Sinninghe Damsté,
704 J.S., 2004. Combined DNA and lipid analyses of sediments reveal changes in Holocene

705 haptophyte and diatom populations in an Antarctic lake. *Earth and Planetary Science*
706 *Letters* 223, 225–239.

707 Coolen, M.J., Boere, A., Abbas, B., Baas, M., Wakeham, S.G., Sinninghe Damsté, J.S., 2006.
708 Ancient DNA derived from alkenone-biosynthesizing haptophytes and other algae in
709 Holocene sediments from the Black Sea. *Paleoceanography* 21, DOI:
710 10.1029/2005PA001188.

711 Coolen, M.J., Saenz, J.P., Giosan, L., Trowbridge, N.Y., Dimitrov, P., Dimitrov, D., Eglinton,
712 T.I., 2009. DNA and lipid molecular stratigraphic records of haptophyte succession in
713 the Black Sea during the Holocene. *Earth and Planetary Science Letters* 284, 610–621.

714 D’Andrea, W.J., Lage, M., Martiny, J.B.H., Laatsch, A.D., Amaral-Zettler, L.A., Sogin, M.L.,
715 Huang, Y., 2006. Alkenone producers inferred from well-preserved 18S rDNA in
716 Greenland lake sediments. *Journal of Geophysical Research Biogeosciences* 111, DOI:
717 10.1029/2005JG000121.

718 Danielssen, D.S., Svendsen, E., Ostrowski, M., 1996. Long-term hydrographic variation in the
719 Skagerrak based on the section Torungen–Hirtshals. *ICES Journal of Marine Science*
720 53, 917–925.

721 Dean Jr, W. E., 1974. Determination of carbonate and organic matter in calcareous sediments
722 and sedimentary rocks by loss on ignition: comparison with other methods. *Journal of*
723 *Sedimentary Research* 44, 242-248.

724 De Leeuw, J. W., van der Meer, F. W., Rijpstra, W. I. C., Schenck, P. A., 1980. On the
725 occurrence and structural identification of long chain unsaturated ketones and
726 hydrocarbons in sediments. *Physics and Chemistry of the Earth*, 12, 211-217.

727 Emeis, K.-C., Struck, U., Blanz, T., Kohly, A., Voß, M., 2003. Salinity changes in the central
728 Baltic Sea (NW Europe) over the last 10000 years. *The Holocene* 13, 411–421.

729 Englebrecht, A.C., Sachs, J.P., 2005. Determination of sediment provenance at drift sites
730 using hydrogen isotopes and unsaturation ratios in alkenones. *Geochimica et*
731 *Cosmochimica Acta* 69, 4253–4265.

732 Frohlich, K., Grabczak, J., Rozanski, K., 1988. Deuterium and oxygen-18 in the Baltic Sea.
733 *Chemical Geology* 72, 77–83.

734 Fujine, K., Yamamoto, M., Tada, R., Kido, Y., 2006. A salinity-related occurrence of a novel
735 alkenone and alkenoate in Late Pleistocene sediments from the Japan Sea. *Organic*
736 *Geochemistry* 37, 1074–1084.

737 Giosan, L., Coolen, M.J., Kaplan, J.O., Constantinescu, S., Filip, F., Filipova-Marinova, M.,
738 Kettner, A.J., Thom, N., 2012. Early anthropogenic transformation of the Danube-Black
739 Sea system. *Scientific Reports* 2, 582.

740 Gustafsson, B.G., Westman, P., 2002. On the causes for salinity variations in the Baltic Sea
741 during the last 8500 years. *Paleoceanography* 17, 12–1.

742 Hay, B.J., 1988. Sediment accumulation in the central western Black Sea over the past 5100
743 years. *Paleoceanography* 3, 491–508.

744 Hyvärinen, H., Donner, J., Kessel, H., Raukas, A., 1988. The Litorina and Limnaea Sea in the
745 northern and central Baltic, in *Problems of the Baltic Sea History. Annales Academiae*
746 *Scientiarum Fennicae* 148, 25–35.

747 Jensen, J.B., 1995. A Baltic Ice Lake transgression in the southwestern Baltic: Evidence from
748 Fakse Bugt, Denmark. *Quaternary International* 27, 59–68.

749 Jensen, J.B., Bennike, O., Witkowski, A., Lemke, W., Kuijpers, A., 1999. Early Holocene
750 history of the southwestern Baltic Sea: the Ancyclus Lake stage. *Boreas* 28, 437–453.

751 Jones, G.A., Gagnon, A.R., 1994. Radiocarbon chronology of Black Sea sediments. *Deep Sea*
752 *Research Part I: Oceanographic Research Papers* 41, 531–557.

753 de Leeuw, J.W., v.d. Meer, F.W., Rijpstra, W.I.C., Schenck, P.A., 1980. On the occurrence
754 and structural identification of long chain unsaturated ketones and hydrocarbons in
755 sediments. *Physics and Chemistry of the Earth* 12, 211–217.

756 Leipe, T., Tauber, F., Vallius, H., Virtasalo, J., Uścińowicz, S., Kowalski, N., Hille, S.,
757 Lindgren, S., Myllyvirta, T., 2011. Particulate organic carbon (POC) in surface
758 sediments of the Baltic Sea. *Geo-Marine Letters* 31, 175–188.

759 Liu, W., Liu, Z., Fu, M., An, Z., 2008. Distribution of the C₃₇ tetra-unsaturated alkenone in
760 Lake Qinghai, China: A potential lake salinity indicator. *Geochimica et Cosmochimica*
761 *Acta* 72, 988–997.

762 Liu, W., G., Liu, Z., H., Wang, H.Y., He, Y.X., Wang, Z., Xu, L.M., 2011. Salinity control on
763 long-chain alkenone distributions in lake surface waters and sediments of the northern
764 Qinghai-Tibetan Plateau, China. *Geochimica et Cosmochimica Acta* 75, 1693–1703.

765 Marlowe, I.T., Green, J.C., Neal, A.C., Brassell, S., C., Course, P.A., 1984. Long chain (n-
766 C₃₇–C₃₉) alkenones in the Prymnesiophyceae. Distribution of alkenones and other
767 lipids and their taxonomic significance. *British Phycological Journal* 19, 203–216.

768 M'boule, D., Chivall, D., Sinke-Schoen, D., Sinninghe Damsté, J.S., Schouten, S., van der
769 Meer, M.T., 2014. Salinity dependent hydrogen isotope fractionation in alkenones
770 produced by coastal and open ocean haptophyte algae. *Geochimica et Cosmochimica*
771 *Acta* 130, 126–135.

772 van der Meer, M.T., Sangiorgi, F., Baas, M., Brinkhuis, H., Sinninghe Damsté, J.S.,
773 Schouten, S., 2008. Molecular isotopic and dinoflagellate evidence for Late Holocene
774 freshening of the Black Sea. *Earth and Planetary Science Letters* 267, 426–434.

775 van der Meer, M.T., Benthien, A., Bijma, J., Schouten, S., Sinninghe Damsté, J.S., 2013.
776 Alkenone distribution impacts the hydrogen isotopic composition of the C_{37:2} and C_{37:3}
777 alkan-2-ones in *Emiliana huxleyi*. *Geochimica et Cosmochimica Acta* 111, 162–166.

778 van der Meer, M.T., Benthien, A., French, K.L., Epping, E., Zondervan, I., Reichart, G.-J.,
779 Bijma, J., Sinninghe Damsté, J.S., Schouten, S., 2015. Large effect of irradiance on
780 hydrogen isotope fractionation of alkenones in *Emiliana huxleyi*. *Geochimica et*
781 *Cosmochimica Acta* 160, 16–24.

782 Moros, M., Lemke, W., Kuijpers, A., Endler, R., Jensen, J.B., Bennike, O., Gingele, F., 2002.
783 Regressions and transgressions of the Baltic basin reflected by a new high-resolution
784 deglacial and postglacial lithostratigraphy for Arkona Basin sediments (western Baltic
785 Sea). *Boreas* 31, 151–162.

786 Müller, P.J., Kirst, G., Ruhland, G., von Storch, I., Rosell-Melé, A., 1998. Calibration of the
787 alkenone paleotemperature index $U^{K'_{37}}$ based on core-tops from the eastern South
788 Atlantic and the global ocean (60 N-60 S). *Geochimica et Cosmochimica Acta* 62,
789 1757–1772.

790 Ono, M., Sawada, K., Shiraiwa, Y., Kubota, M., 2012. Changes in alkenone and alkenoate
791 distributions during acclimatization to salinity change in *Isochrysis galbana*:
792 Implication for alkenone-based paleosalinity and paleothermometry. *Geochemical*
793 *Journal* 46, 235–247.

794 Pahl, F.G., Wakeham, S.G., 1987. Calibration of unsaturation patterns in long-chain ketone
795 compositions for palaeotemperature assessment. *Nature* 330, 367-369.

796 Pahl, F.G., Muehlhausen, L.A., Zahnle, D.L., 1988. Further evaluation of long-chain
797 alkenones as indicators of paleoceanographic conditions. *Geochimica et Cosmochimica*
798 *Acta* 52, 2303–2310.

799 Pahl, F.G., Rontani, J.-F., Volkman, J.K., Sparrow, M.A., Royer, I.M., 2006. Unusual C_{35}
800 and C_{36} alkenones in a paleoceanographic benchmark strain of *Emiliana huxleyi*.
801 *Geochimica et Cosmochimica Acta* 70, 2856–2867.

802 Punning, J., Martma, T., Kessel, H., Vaikme, R., 1988. The isotopic composition of oxygen
803 and carbon in the subfossil mollusc shells of the Baltic Sea as an indicator of
804 palaeosalinity. *Boreas* 17, 27–31.

805 Randlett, M.-E., Coolen, M.J., Stockhecke, M., Pickarski, N., Litt, T., Balkema, C., Kwiecien,
806 O., Tomonaga, Y., Wehrli, B., Schubert, C.J., 2014. Alkenone distribution in Lake Van
807 sediment over the last 270 ka: Influence of temperature and haptophyte species
808 composition. *Quaternary Science Review* 104, 53–62.

809 Rechka, J.A., Maxwell, J.R., 1988. Characterisation of alkenone temperature indicators in
810 sediments and organisms. *Organic Geochemistry* 13, 727–734.

811 Rosell-Melé, A., 1998. Interhemispheric appraisal of the value of alkenone indices as
812 temperature and salinity proxies in high-latitude locations. *Paleoceanography* 13, 694–
813 703.

814 Ross, D.A., Degens, E.T., MacIlvaine, J., 1970. Black Sea: recent sedimentary history.
815 *Science* 170, 163–165.

816 Rößler, D., Moros, M., Lemke, W., 2011. The Littorina transgression in the southwestern
817 Baltic Sea: new insights based on proxy methods and radiocarbon dating of sediment
818 cores. *Boreas* 40, 231–241.

819 Ryan, W.B., Pitman, W.C., Major, C.O., Shimkus, K., Moskalenko, V., Jones, G.A.,
820 Dimitrov, P., Görür, N., Sakiñç, M., Yüce, H., 1997. An abrupt drowning of the Black
821 Sea shelf. *Marine Geology* 138, 119–126.

822 Schouten, S., Ossebaar, J., Schreiber, K., Kienhuis, M.V.M., Langer, G., Bijma, J., 2005. The
823 effect of temperature and salinity on the stable hydrogen isotopic composition of long
824 chain alkenones produced by *Emiliania huxleyi* and *Gephyrocapsa oceanica*.
825 *Biogeosciences* 2, 1681–1695.

826 Schulz, H.-M., Schöner, A., Emeis, K.-C., 2000. Long-chain alkenone patterns in the Baltic
827 Sea—an ocean-freshwater transition. *Geochimica et Cosmochimica Acta* 64, 469–477.

828 Sikes, E.L., Sicre, M.-A., 2002. Relationship of the tetra-unsaturated C₃₇ alkenone to salinity
829 and temperature: Implications for paleoproxy applications. *Geochemistry, Geophysics,
830 Geosystems* 3, 1–11.

831 Song, M., Zhou, A., He, Y., Zhao, C., Wu, J., Zhao, Y., Liu, W., Liu, Z., 2016. Environmental
832 controls on long-chain alkenone occurrence and compositional patterns in lacustrine
833 sediments, northwestern China. *Organic Geochemistry* 91, 43–53.

834 Sun, Q., Chu, G., Liu, G., Li, S., Wang, X., 2007. Calibration of alkenone unsaturation index
835 with growth temperature for a lacustrine species *Chrysothila lamellosa* (Haptophyceae).
836 *Organic Geochemistry* 38, 1226–1234.

837 Swart, P.K., 1991. The oxygen and hydrogen isotope composition of the Black Sea. *Deep-Sea
838 Research* 38, S761-S772.

839 Thiel, V., Jenisch, A., Landmann, G., Reimer, A., Michaelis, W., 1997. Unusual distributions
840 of long-chain alkenones and tetrahymanol from the highly alkaline Lake Van, Turkey.
841 *Geochimica et Cosmochimica Acta* 61, 2053–2064.

842 Tikkanen, M., Oksanen, J., 2002. Late Weichselian and Holocene shore displacement history
843 of the Baltic Sea in Finland. *Fennia-International Journal of Geography* 180, 9–20.

844 Van Soelen, E.E., Lammers, J.M., Eglinton, T.I., Sinninghe Damsté, J.S., Reichart, G.J.,
845 2014. Unusual C₃₅ to C₃₈ alkenones in mid-Holocene sediments from a restricted
846 estuary (Charlotte Harbor, Florida). *Organic Geochemistry* 70, 20–28.

847 Volkman, J.K., Eglinton, G., Corner, E.D., Forsberg, T.E.V., 1980. Long-chain alkenes and
848 alkenones in the marine coccolithophorid *Emiliania huxleyi*. *Phytochemistry* 19, 2619–
849 2622.

850 Volkman, J.K., Barrerr, S.M., Blackburn, S.I., Sikes, E.L., 1995. Alkenones in *Gephyrocapsa*
851 *oceanica*: Implications for studies of paleoclimate. *Geochimica et Cosmochimica Acta*
852 59, 513–520.

853 Westman, P., Sohlenius, G., 1999. Diatom stratigraphy in five offshore sediment cores from
854 the northwestern Baltic proper implying large scale circulation changes during the last
855 8500 years. *Journal of Paleolimnology* 22, 53–69.

856 Winterhalter, B., 1992. Late-Quaternary stratigraphy of Baltic Sea basins—a review. *Bulletin*
857 *of the Geological Society Finland* 64, 189–194.

858 Witkowski, A., Broszinski, A., Bennike, O., Janczak-Kostecka, B., Jensen, J.B., Lemke, W.,
859 Endler, R., Kuijpers, A., 2005. Darss Sill as a biological border in the fossil record of
860 the Baltic Sea: evidence from diatoms. *Quaternary International* 130, 97–109.

861 Wolhowe, M.D., Prah, F.G., Langer, G., Oviedo, A.M., Ziveri, P., 2015. Alkenone δD as an
862 ecological indicator: A culture and field study of physiologically-controlled chemical
863 and hydrogen-isotopic variation in C₃₇ alkenones. *Geochimica et Cosmochimica Acta*
864 162, 166–182.

865 Xu, L., Reddy, C.M., Farrington, J.W., Frysinger, G.S., Gaines, R.B., Johnson, C.G., Nelson,
866 R.K., Eglinton, T.I., 2001. Identification of a novel alkenone in Black Sea sediments.
867 *Organic Geochemistry* 32, 633–645.

868 Zheng, Y., Huang, Y., Andersen, R.A., Amaral-Zettler, L.A., 2016. Excluding the di-
869 unsaturated alkenone in the UK₃₇ index strengthens temperature correlation for the
870 common lacustrine and brackish-water haptophytes. *Geochimica et Cosmochimica Acta*
871 175, 36–46.

872 Zink, K.-G., Leythaeuser, D., Melkonian, M., Schwark, L., 2001. Temperature dependency of
873 long-chain alkenone distributions in recent to fossil limnic sediments and in lake waters.
874 *Geochimica et Cosmochimica Acta* 65, 253–265.

876 **Figure legends**

877 **Figure 1** A map of the Baltic Sea region and sampling sites. The sediment coring sites
878 318310 and 318340 in the Arkona Basin are designated by blue circles and the two stations in
879 the Skagerrak where surface sediment samples were collected are indicated by red squares.

880 **Figure 2** Correlation of sediment cores 318310 (left panel) and 318340 (right panel) using Ca
881 data obtained from XRF analysis (cps; designated by the gold line) and LOI (wt%; designated
882 by the black line). The red numbers indicate the radiocarbon dates (in cal yr BP) of carbonate
883 fossils from specific horizons in core 318310. The blue lines indicate tie points used for
884 correlating both cores (see text). The closed circles along the depth axes indicate the depths of
885 the sediments analyzed for alkenones in this study.

886 **Figure 3** Partial GC-FID chromatograms displaying alkenone distribution from various
887 sediment horizons. (a) Sample EMB0461-10-MUC from the Skagerrak shows a typical
888 marine distribution, (b) a sediment interval from 0.4 cal kyr BP (50 cm depth from core
889 318310) is from a brackish period and displays a distribution similar to the marine distribution
890 except with the additional presence of the $C_{36:2}$ alkenone, (c) the sediment interval from 0.9
891 cal kyr BP (100 cm depth from core 318310) has a different distribution from the other depths
892 in both cores with no $C_{37:4}$ alkenone, $C_{37:3} < C_{37:2}$, and a lower contribution of the $C_{36:2}$
893 alkenone relative to the C_{37} alkenones, (d) the sediment interval from 7.1 cal kyr BP (600 cm
894 depth from core 318310) is from the period immediately following the Ancyclus
895 Lake/Littorina Sea transition and has an alkenone distribution characteristic of lower salinity
896 haptophytes. Note the high relative abundance of the $C_{36:2}$ alkenone at this time. The
897 alkenones are color coded according to the legend with circles designating the C_{38} alkenones,
898 triangles signifying the $C_{36:2}$ alkenone, and squares indicating the C_{37} alkenones.

899 **Figure 4** Principal component analysis based on the standardized fractional abundances of the
900 eight alkenones found consistently in the sediments from the Baltic Sea used in this study.
901 Samples where alkenones were not detected were left out of the PCA. (a) Plot showing the
902 scores of the alkenones and scores of the different sites on PC1 (41.0%) and PC2 (25.6%). (b)
903 Displays the scores of the alkenones on PC1 ac PC3 (18.1%) as well as the scores of the
904 different sites. Scatter plots displaying the correlation of (c) PC1 with $U^{K'}_{37}$ ($R^2=0.86$) (d)
905 negative correlation of PC2 and $C_{36:2}$ Et ($R^2=0.77$) (e) and negative correlation with PC3 and
906 the sum of the C_{38} Et ($R^2=0.74$).

907 **Figure 5** Plots of the combined Arkona Basin record (sediment core 318310 designated by
908 closed symbols and 318340 by open symbols) with age (cal kyr BP) for (a) PC1-PC3 (b)
909 summed fractional abundance of the C_{38} Et alkenones, (c) fractional abundance of the $C_{36:2}$
910 alkenone (%) (d) $\%C_{37:4}$, and (e) $U^{K'}_{37}$.

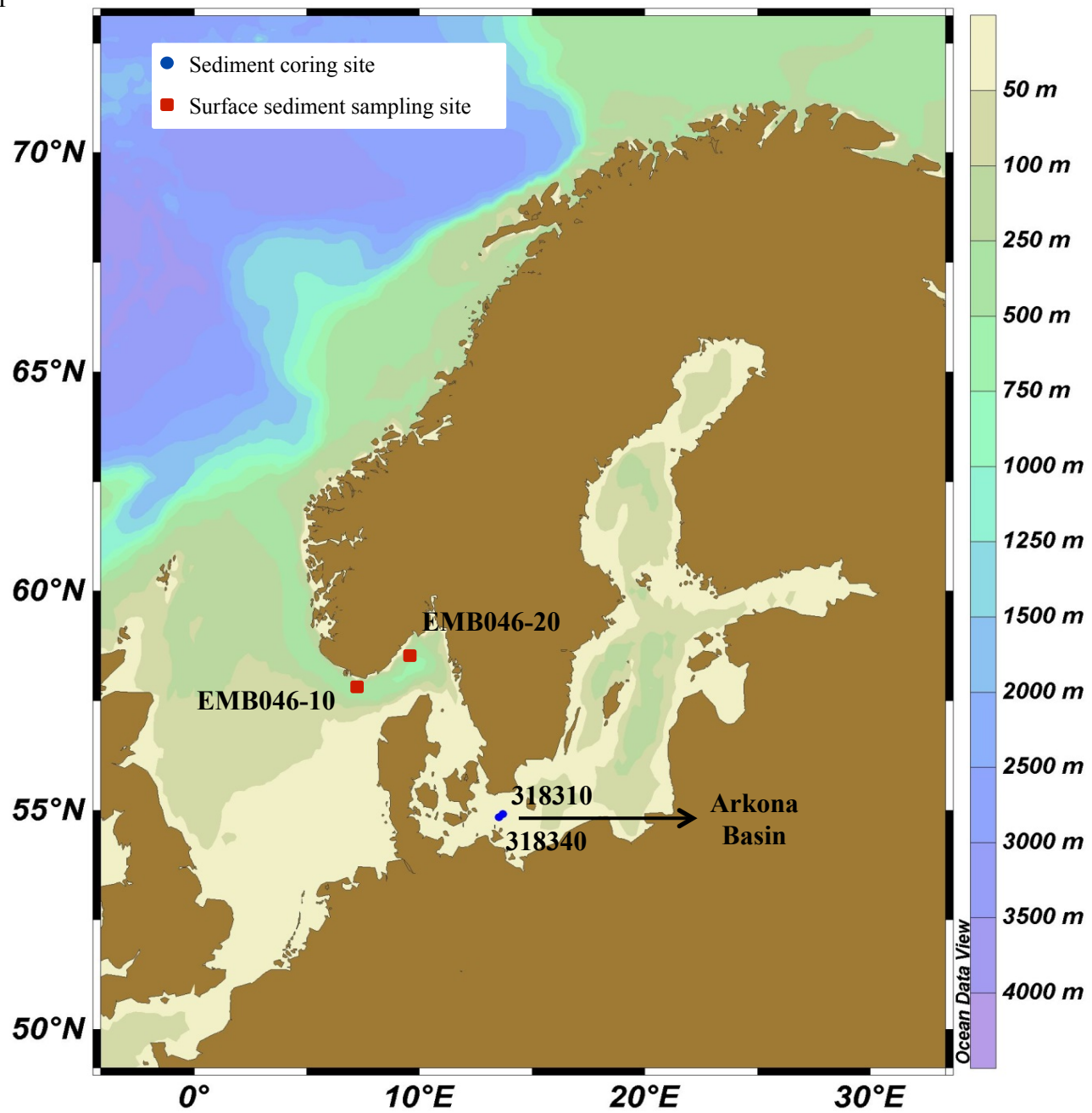
911 **Figure 6** δD values of the $C_{36:2}$, C_{37} and C_{38} alkenones plotted against age (cal kyr BP) from
912 the record 318310 and the two Skagerrak surface sediment samples. In the Arkona Basin
913 conditions were fresh until 7.8 cal kyr BP and brackish from 7.1 cal kyr BP onwards. The
914 sample points in black are for sediments from the Arkona Basin record (sediment core
915 318310) and the red sample points are for the Skagerrak surface sediments. The circles denote
916 the δD of the $C_{36:2}$ alkenones, the squares signify the δD values C_{37} alkenones and the
917 diamonds represent the δD of the C_{38} alkenones.

918 **Figure 7** Comparison of $C_{36:2}$ alkenone abundance data for the Baltic Sea and the Black Sea
919 over the Holocene. Top panel (a) shows the fractional abundance of the $C_{36:2}$ alkenone
920 relative to the C_{36} - C_{38} alkenones for the Black Sea (blue circles; data from Coolen et al., 2009)
921 and Baltic Sea (green triangles; this study). The middle panel (b) shows the haptophyte
922 community composition in the Black Sea as reconstructed based on DGGE analysis of partial

923 18S rRNA genes amplified with a specific haptophyte primer set with *Isochrysis*-related
924 haptophytes in red and *E. huxleyi* in blue (data modified from Coolen et al., 2009; note that in
925 their Fig. 3 relative abundance data is shown based on the relative abundance of all DGGE
926 bands not only those related to alkenone-producing haptophytes, Coolen, personal
927 communication). These data are in agreement with earlier haptophyte 18S rRNA gene work
928 on a box core just penetrating Unit 2 from a deep water site in the eastern Black Sea (Coolen
929 et al., 2006). The bottom panel (c) shows reconstructed salinities for the Black Sea based on
930 the hydrogen isotopic compositions of the C_{36:2} and C₃₇ alkenones. For all data the
931 fractionation factor α was calculated using a water hydrogen isotopic composition of -20
932 permille (Swart, 1991). Salinities were reconstructed based on the α -salinity relationship for
933 *Isochrysis galbana* ($\alpha=0.0019*S+0.836$; M'Boule et al., 2014) for the C_{36:2} alkenone and *E.*
934 *huxleyi* ($\alpha=0.0021*S+0.740$; M'Boule et al., 2014) for the C₃₇ alkenones. Original alkenone
935 hydrogen isotope data are for the eastern Black Sea from van der Meer et al. (2008) and for
936 the western Black Sea from Giosan et al. (2012). The stratigraphy for the Baltic Sea (top) and
937 Black Sea (bottom) is indicated. TS denotes transition sapropel. Note that the stratigraphy
938 described for the Black Sea core in the study of Coolen et al. (2009) and Giosan et al. (2012)
939 has been adjusted to fit the commonly applied stratigraphy for the Black Sea (see lowermost
940 part of the figure), i.e. the layer of the first invasion of *E. huxleyi* (grey bar in the other panels)
941 is taken as the start of Unit 1 deposition (Hay et al., 1992; Arthur et al. 1994; Jones and
942 Gagnon, 1994). In the sediment core used in the work of Coolen et al. (2009) this layer is not
943 clearly revealed by an increase of the carbonate content but the alkenone distribution shows a
944 distinct change at ca. 3,350 cal yr BP (see sudden decrease of the relative abundance of the
945 C_{36:2} alkenone in panel a; in addition this horizon is also characterized by a 3-4 fold increase
946 in total alkenone concentration and the detection of C₃₉ alkenones; Coolen et al., 2009)
947 towards a composition highly comparable to the upper part of Unit I that is composed of

948 coccolithic ooze. Their reported radiocarbon date for this section ($3,360 \pm 68$ cal yr BP) is by
949 this adjustment in good agreement with the reported age of the base of Unit I at other
950 locations in the Black Sea (Hay et al., 1992; Arthur et al. 1994; Jones and Gagnon, 1994).

Figure 1



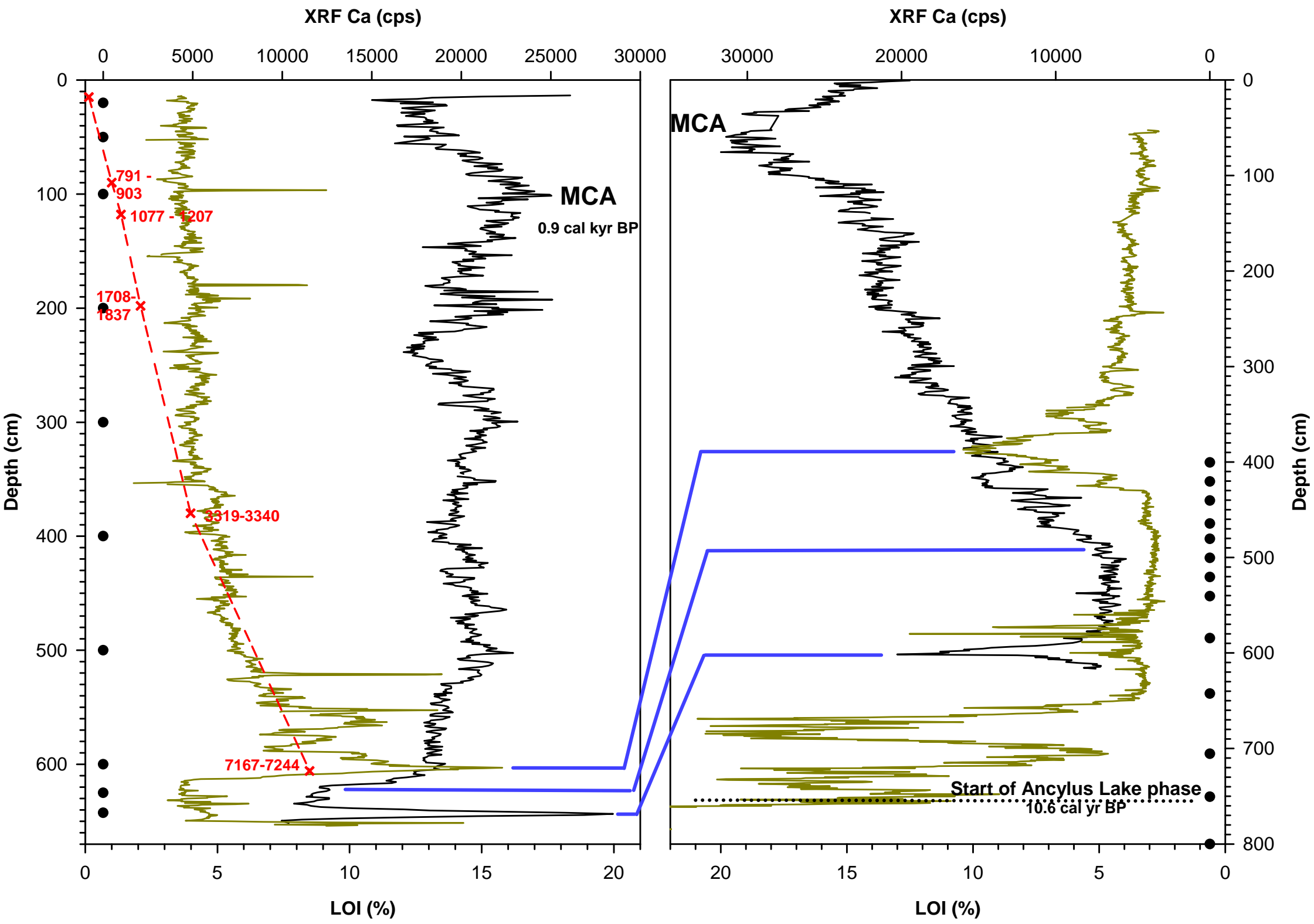


Figure 3

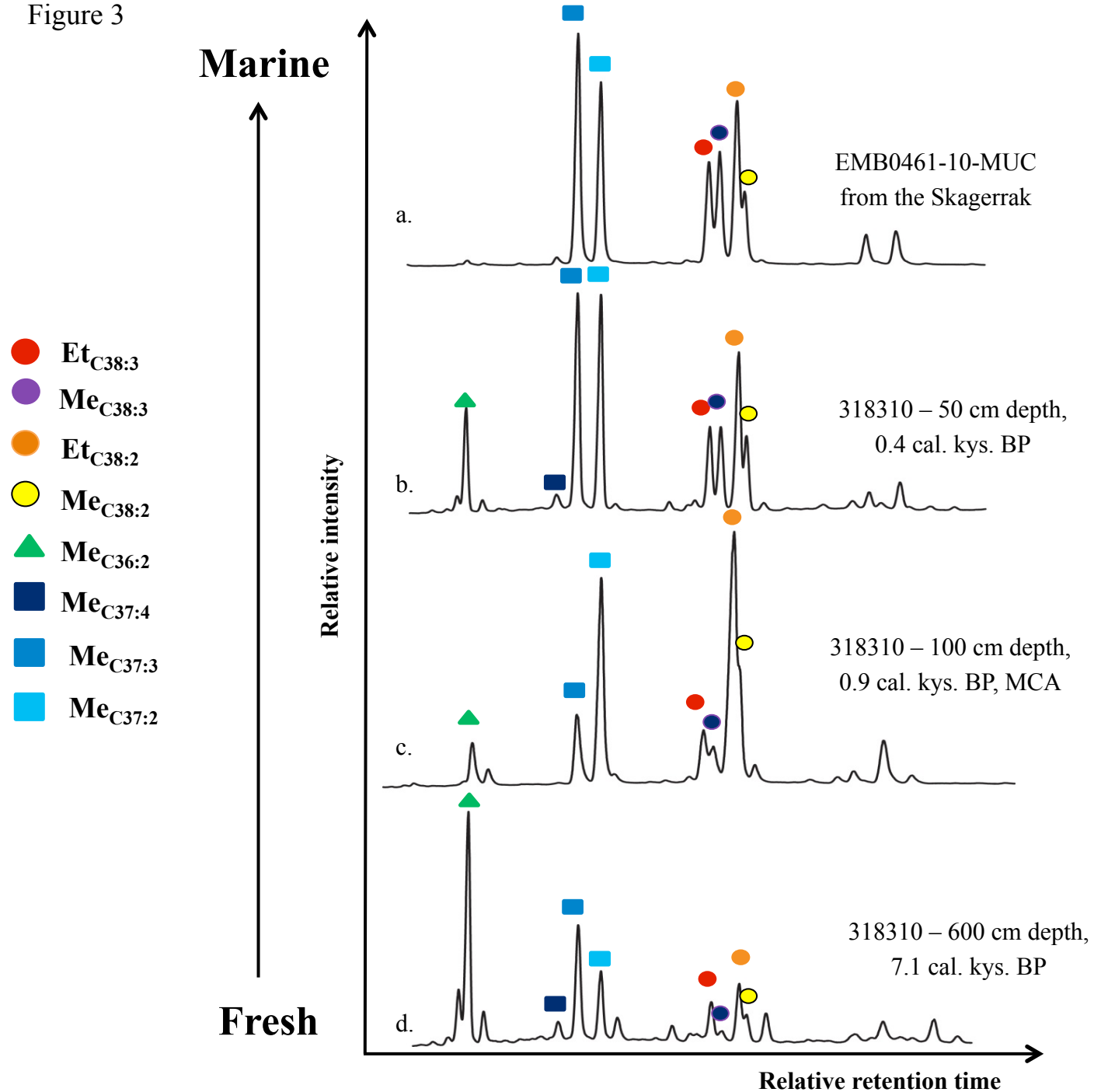


Figure 4

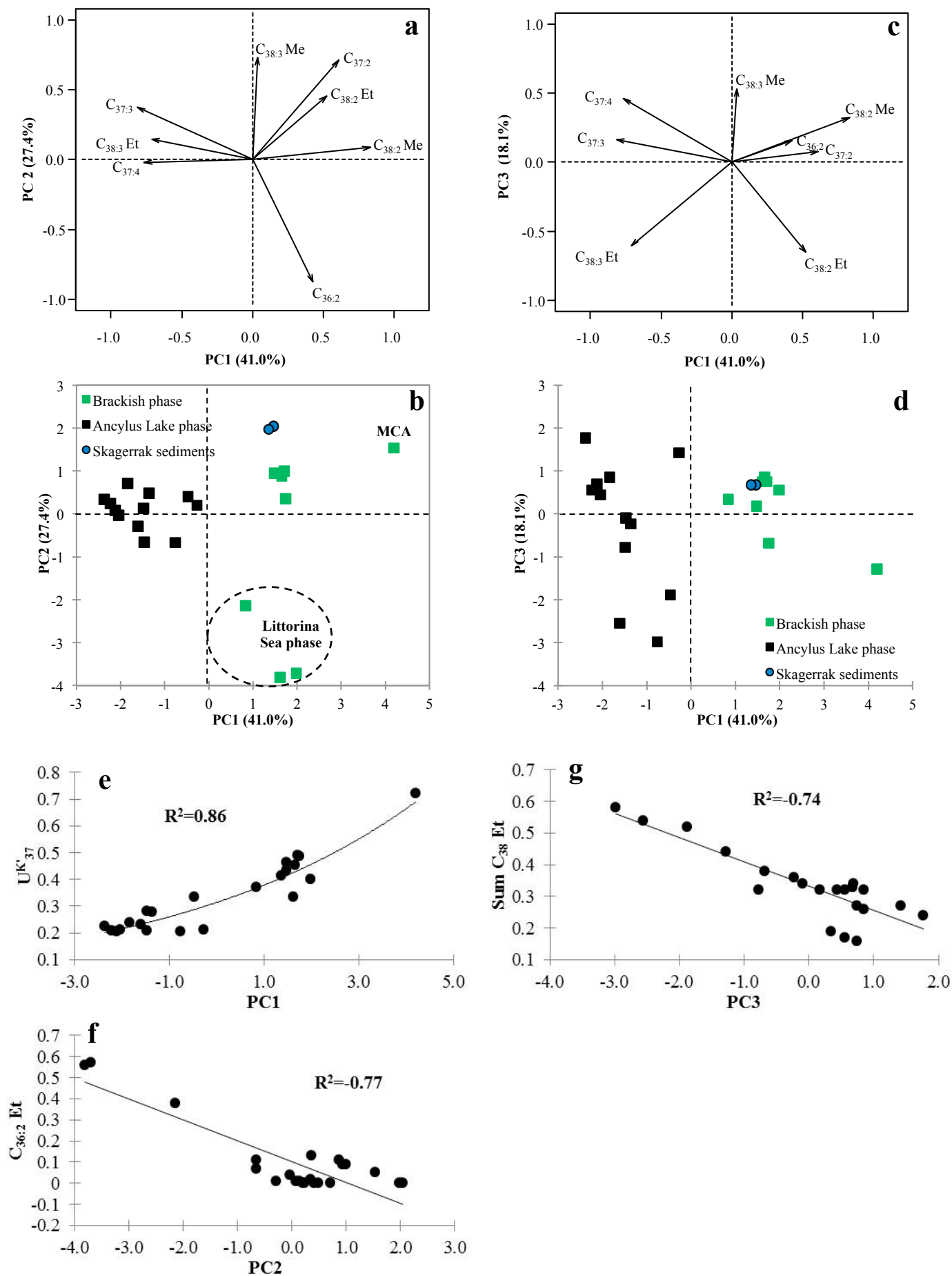


Figure 5

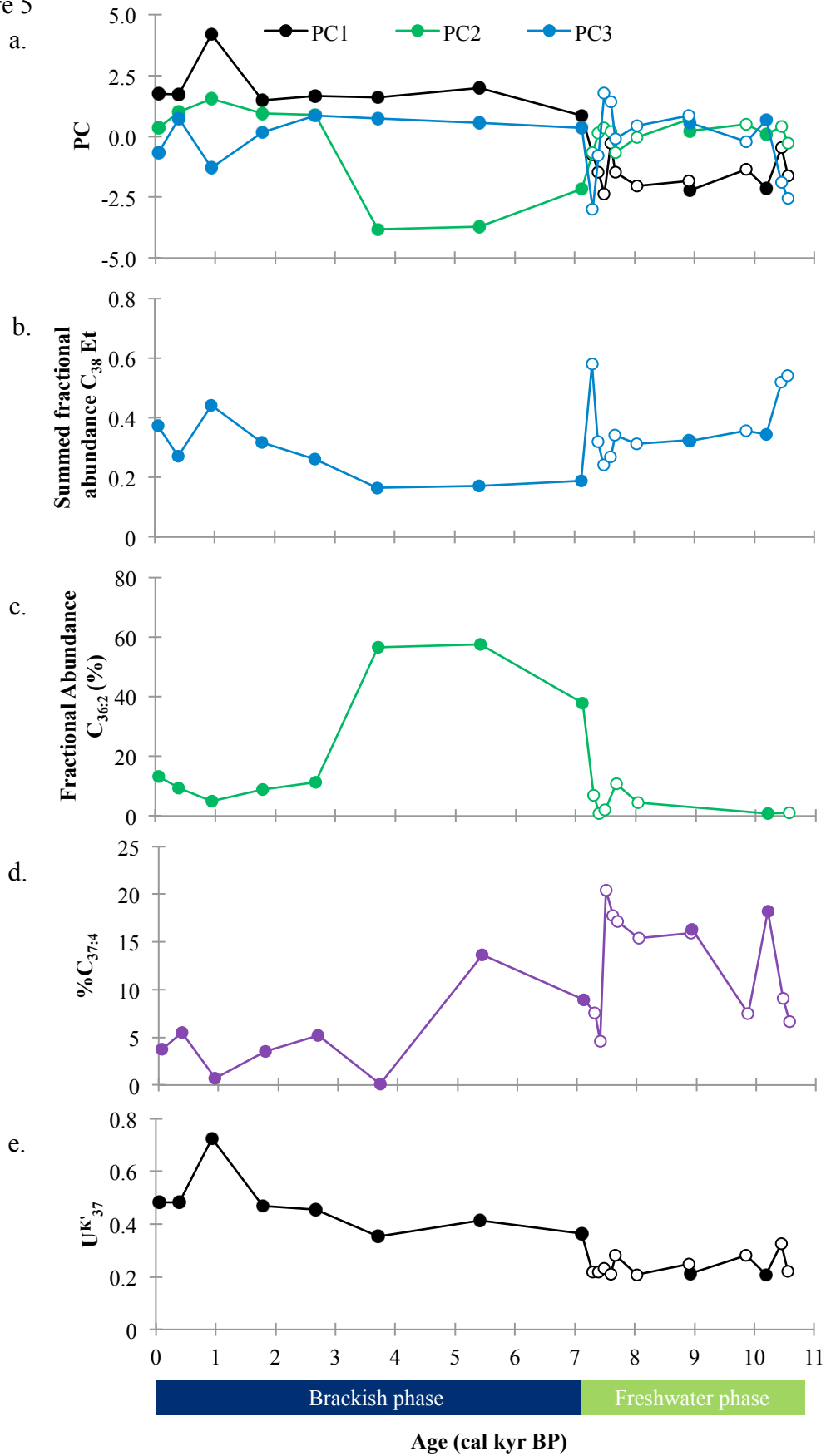
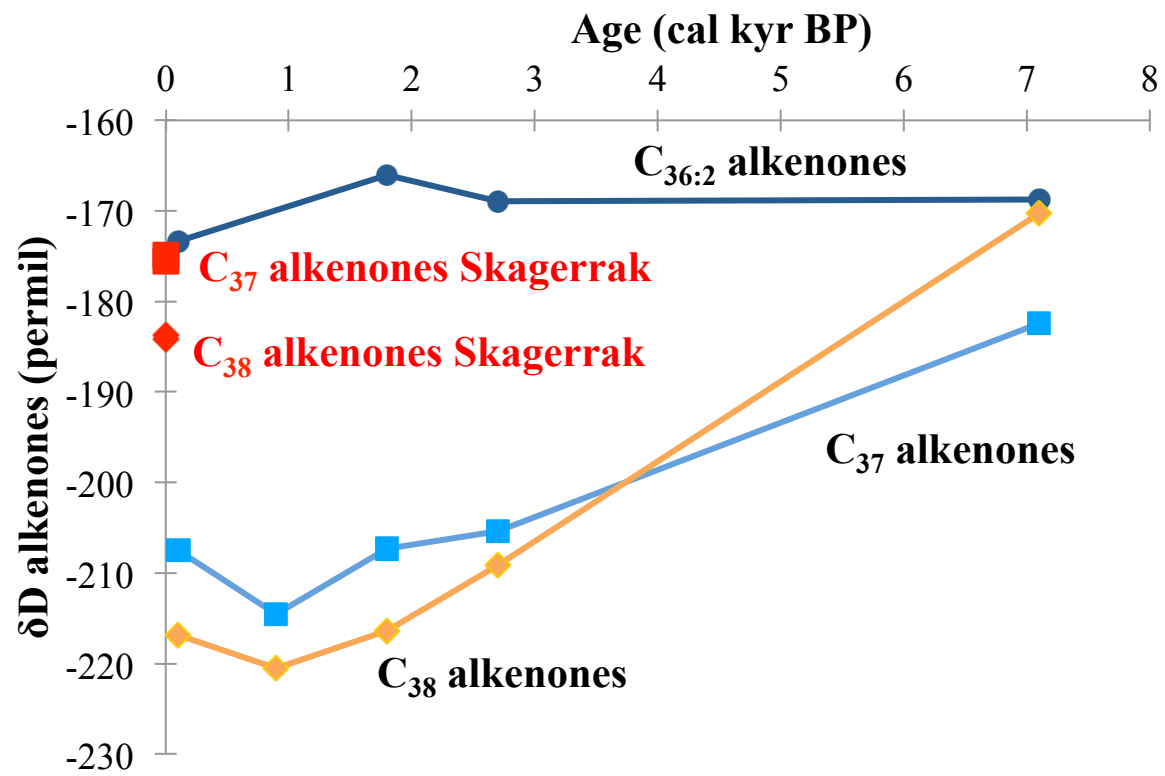
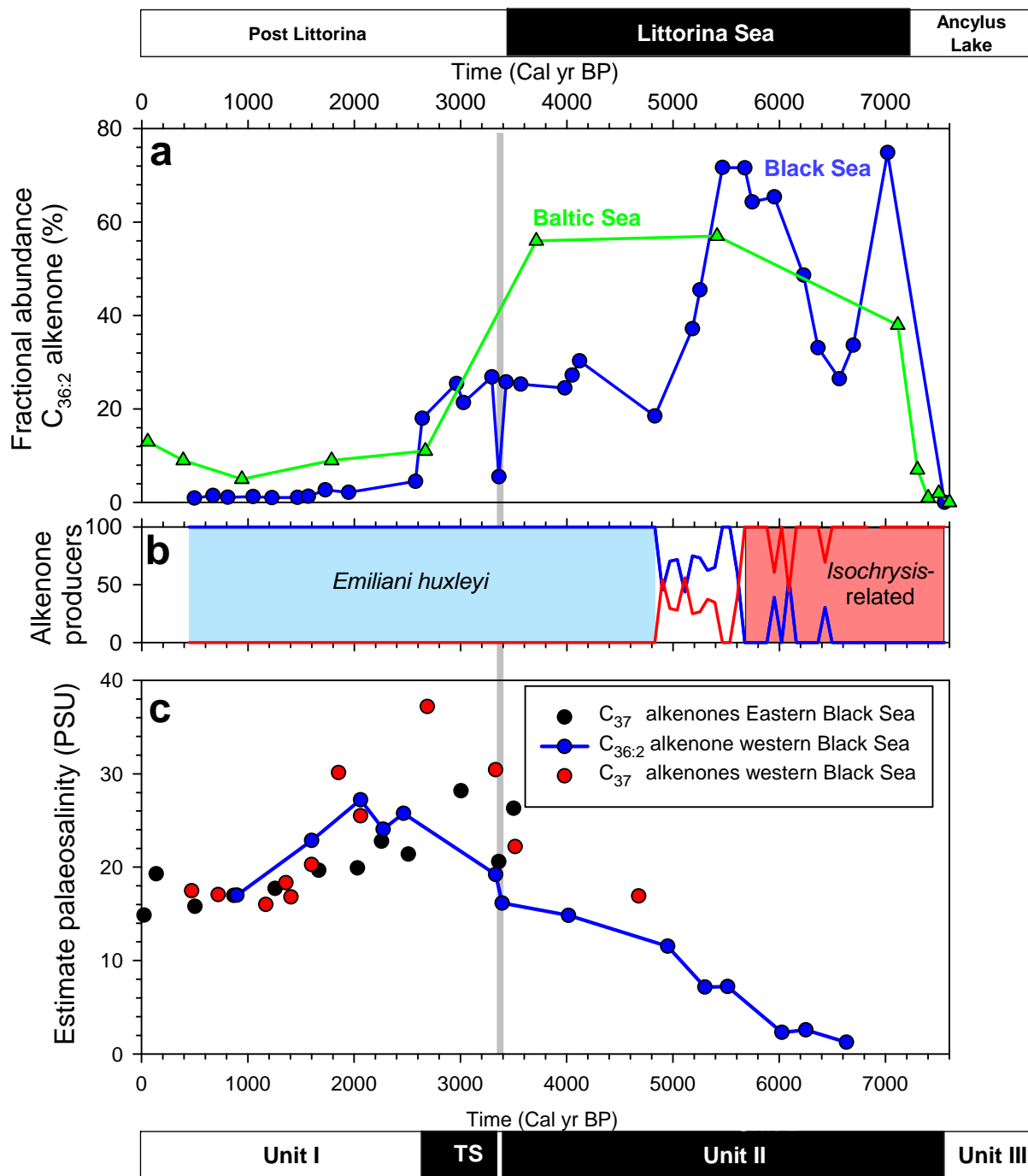


Figure 6:



Baltic Sea



Black Sea